

# 地表能量平衡的长期变化及其对气温变化的影响

王开存 ([kcwang@bnu.edu.cn](mailto:kcwang@bnu.edu.cn))

北京师范大学

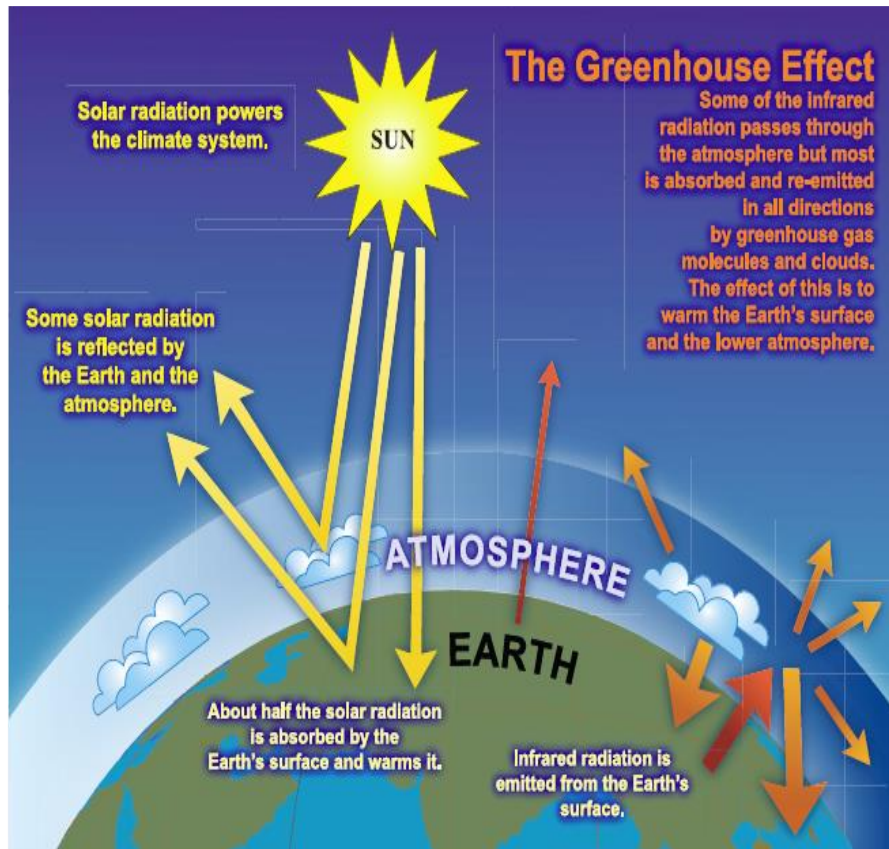
# 能量收支决定了气候变化方向和强度

- 太阳短波辐射是地球气候系统的能量来源。
- 地球气候系统发射长波辐射以维持能量平衡，保持温度基本不变。
- 大气顶能量平衡方程

$$S_0 \cdot \pi \cdot R^2 \cdot (1 - \alpha) = 4 \cdot \pi \cdot R^2 \cdot \sigma \cdot T_{eff}^4$$

- $T_{eff} \approx 255 \text{ K}$  ( $-18^\circ\text{C}$ )为地球气候系统的有效温度，可以理解为对流层上层或平流层的温度。
- 全球平均地表气温为 $\sim 15^\circ\text{C}$ 。

# 大气的温室效应



- 除紫外波段外，大气对太阳短波辐射几乎是透明的。
- 水汽，CO<sub>2</sub>等温室气体和云吸收地表发射的长波辐射，同时向各个方向发射长波辐射。
- 温室气体浓度的增加，降低了地表向外发射长波辐射的能力，对地表有保温效应（即温室效应），但对中上层大气有降温作用。

# 为什么CO<sub>2</sub>是讨论最多的温室气体？

- CO<sub>2</sub>等长生命周期的温室气体不易清除，在大气中的留存时间在百年以上，在大气中混合均匀。
- 水汽是最重要的温室气体。温室气体浓度的增加，对近地面大气有增温作用。大气中的水汽含量随气温的增加指数增加（水汽的正反馈效应）。
- 如果能够清除空气中CO<sub>2</sub>，气温会随之降低。温度降低，空气中的水汽达到饱和点后会凝结，通过云雨过程降落地面。

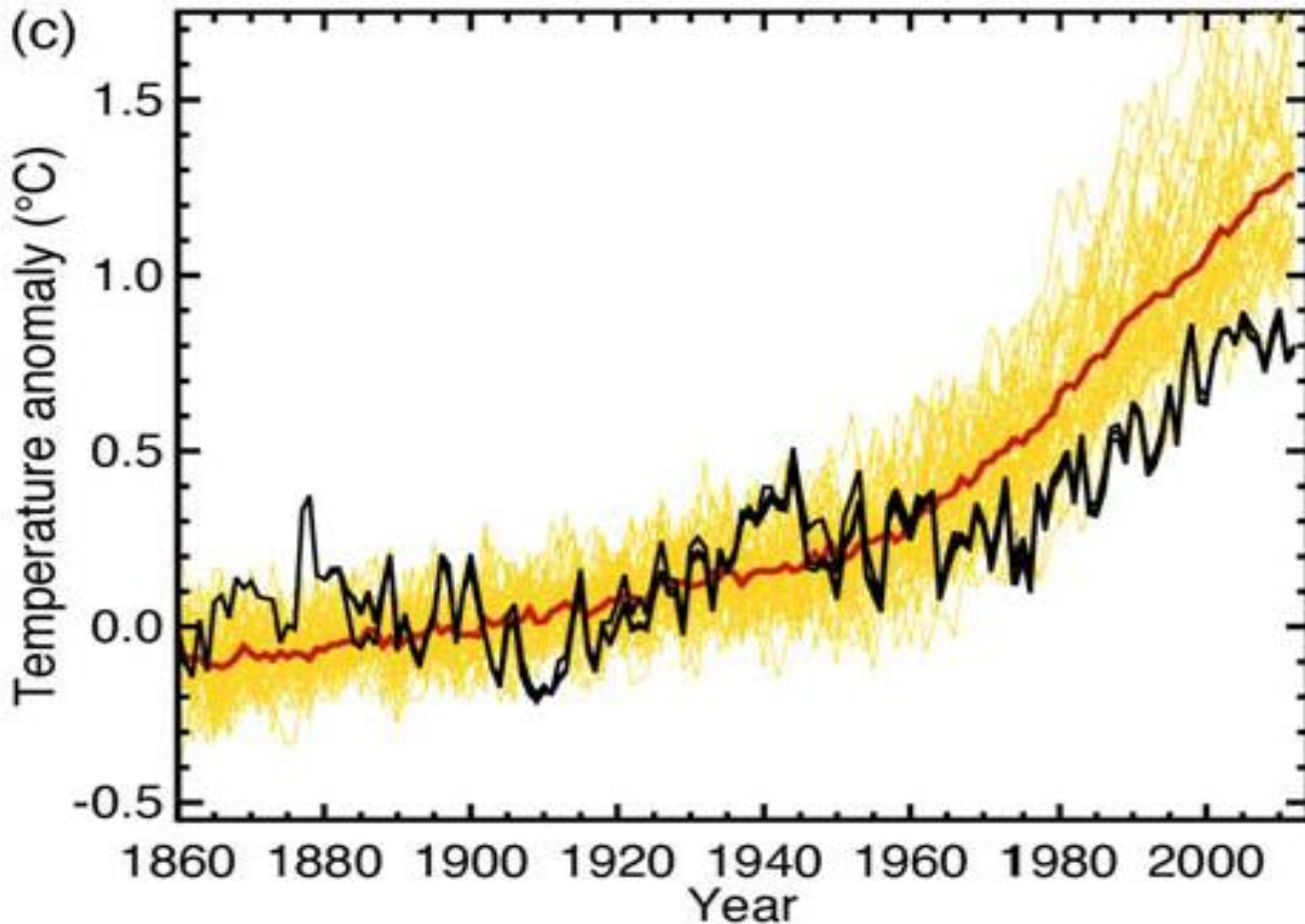
# 全球能量不平衡与增温

- 观测表明最近几十年大气顶净辐射为正：

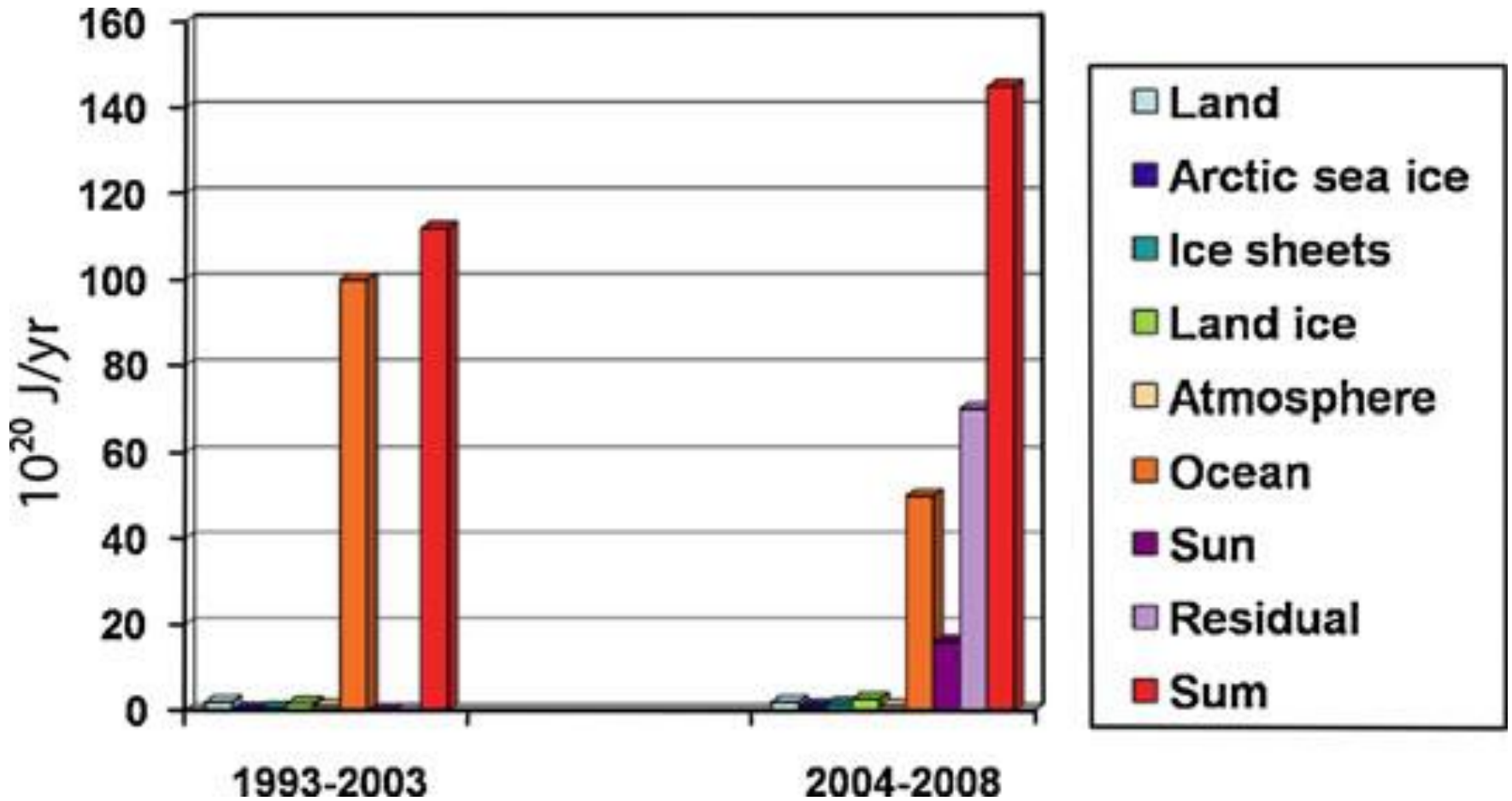
$$Net = S_0 \cdot \pi \cdot R^2 \cdot (1 - \alpha) - 4 \cdot \pi \cdot R^2 \cdot \sigma \cdot T_{eff}^4$$

- 观测表明对流层顶层和平流层的温度有变冷的趋势，即地球系统获得能量，主要因为  $T_{eff}$  降低了。
- 同时地表气温增加（全球变暖），这种对流层低层和平流层相反的温度变化趋势从一个方面说明全球变暖与温室效应有关。
- 但地表气温增加的幅度还与其它很多因素有关，因为：（1）净辐射主要被储存在海洋里（~93%），小部分用来加热大气（~1%）；（2）地表温度的变化还与多种反馈效应有关，这些反馈效应有不同的时间尺度，产生不同地球系统内部变率。

# 实测地表温度变化（黑线） 与温室气体产生的变化（红线）



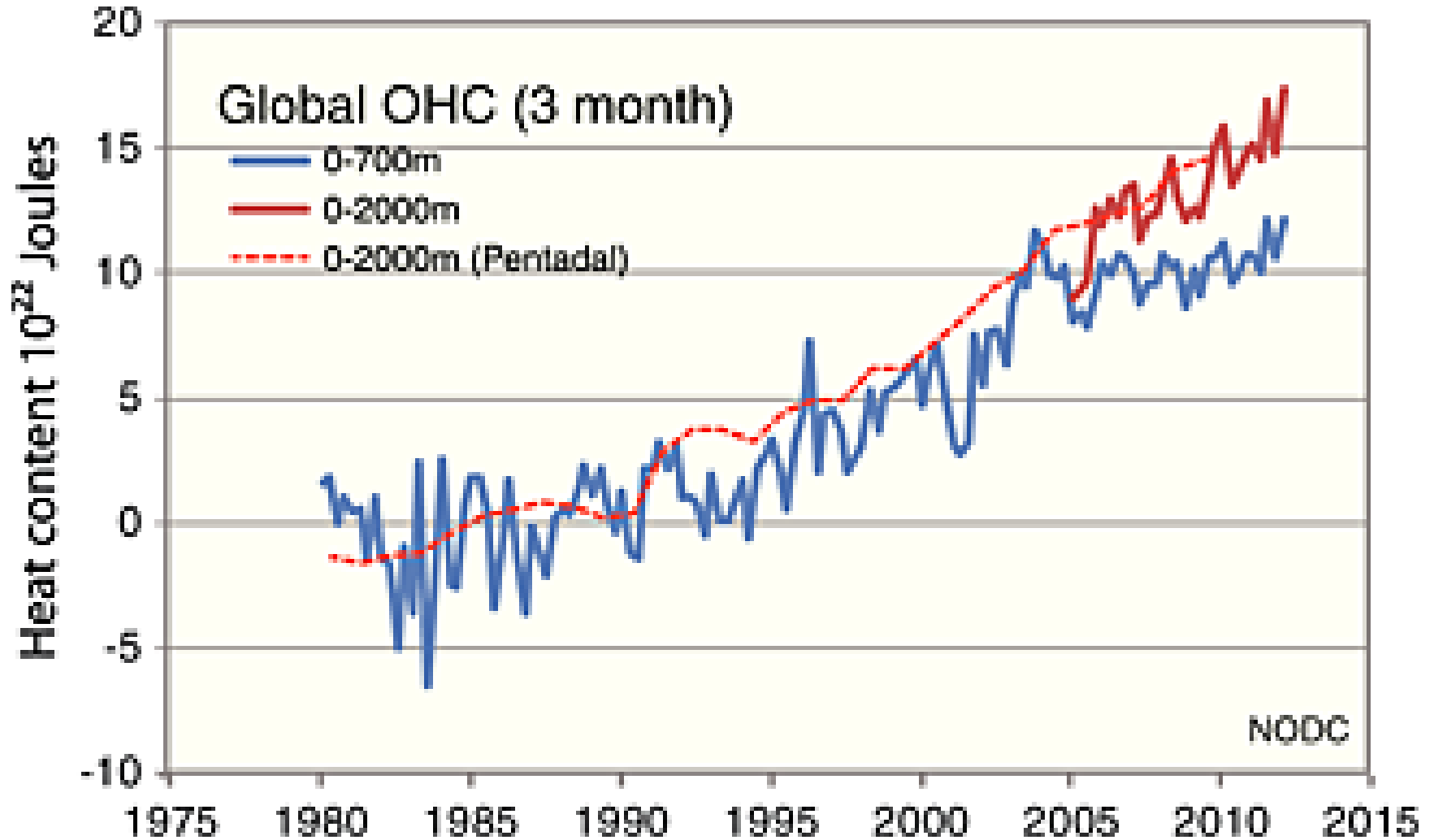
# 地球系统各系统净能量收支



$1.61 \times 10^{22}$  J/yr =  $1 \text{ W m}^{-2}$

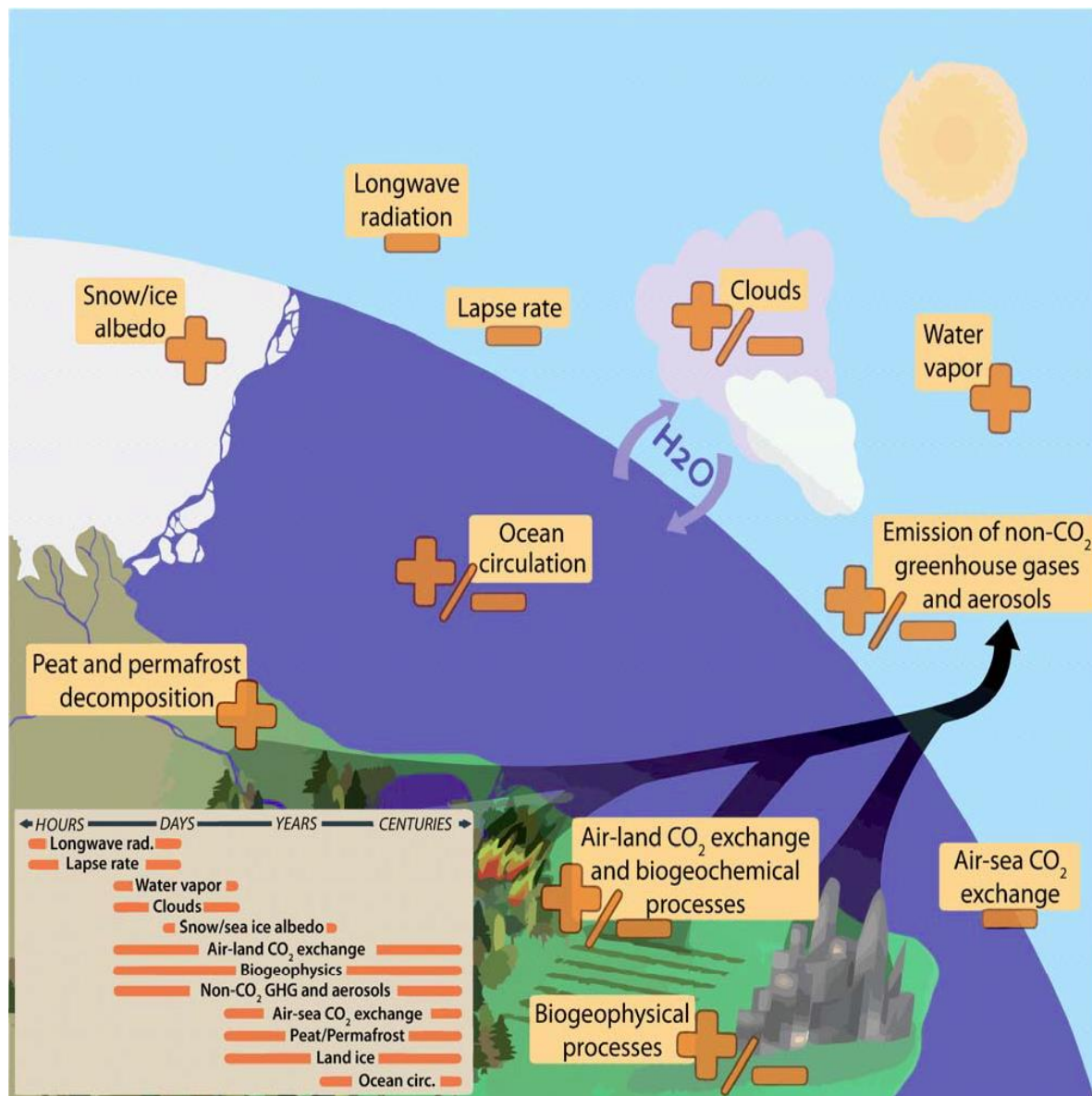
Trenberth, 2011

# 全球海洋热含量的变化





# 温室效应与反馈效应



地表气温随温室气体气体的增加而增加，但增温速率在很大程度上取决于各种反馈效应，这些反馈效应具有不同的时间尺度。

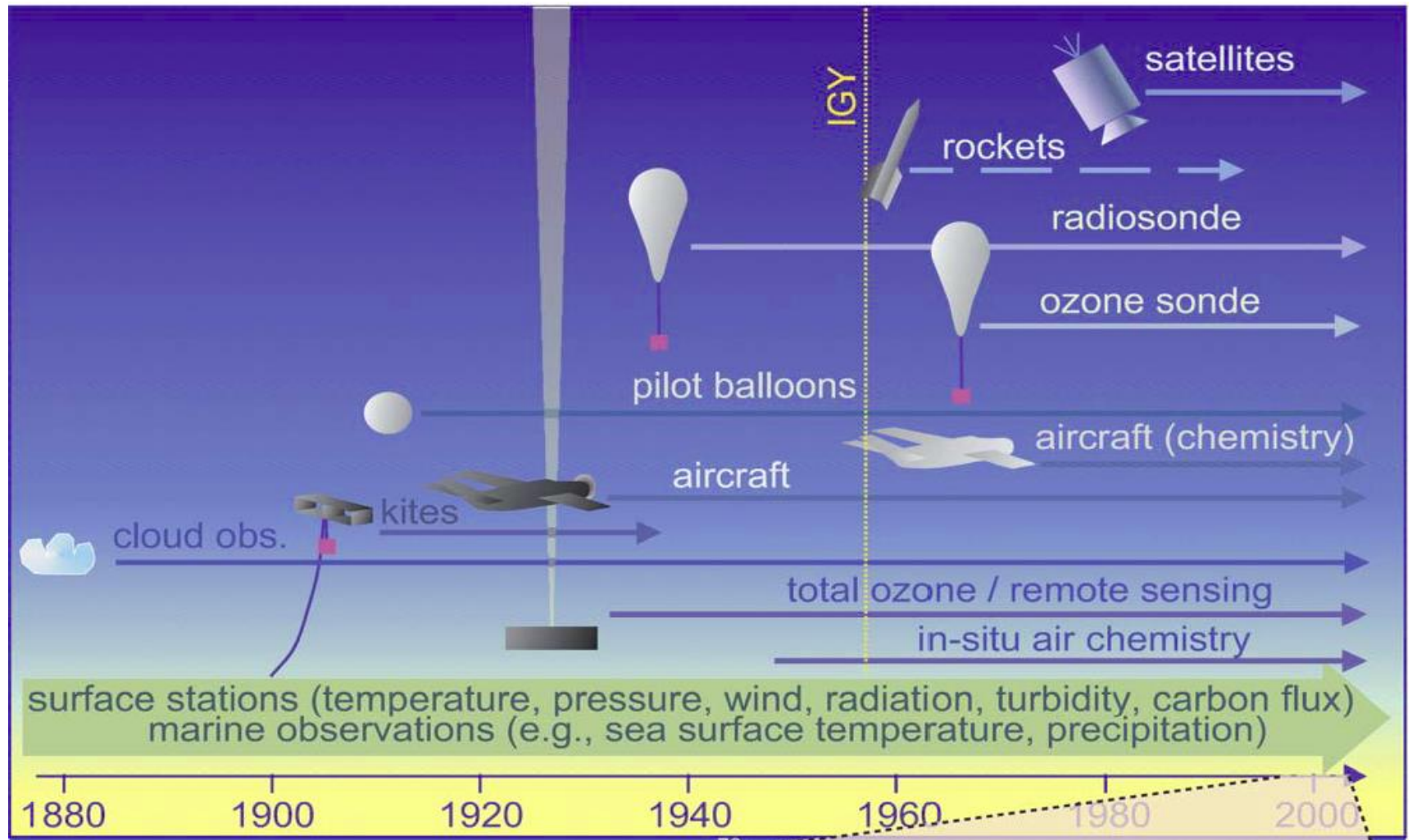
# 地表能量更为复杂

- 地表能量平衡方程：

$$R_n = S_{\downarrow} - S_{\uparrow} + L_{\downarrow} - L_{\uparrow} = G + H + LE$$

- 地表入射太阳辐射受云和气溶胶的影响，反射太阳辐射与地表状况有关。大气向下长波辐射表征温室效应的强度，与地表气温有关。地表发射辐射取决于地表温度。
- LE为潜热通量，E为蒸散（植被蒸腾加蒸发），它连接着地表能量平衡和水平衡。
- 地表净辐射在感热和潜热之间的分配决定了地表对大气的加热强度，可以提供多少水汽，影响云和降水过程。
- 水汽凝结过程释放的潜热，影响降水强度和降雨量，为大气环流提供能量。

# 地表能量平衡各参量不是常规观测项目



# 地表能量平衡缺乏直接观测资料

- 从1958年开始，少数气象站开始使用总辐射表观测地表入射太阳辐射，1990年代以后改进了观测方式。
- 20世纪90年代以后一些研究站点开始观测气溶胶光学厚度、长波辐射、感热和潜热通量。但这些观测并不能提供这些量的区域或全球平均变化情况。

# 地表能量平衡各分量的长期变化情况如何？

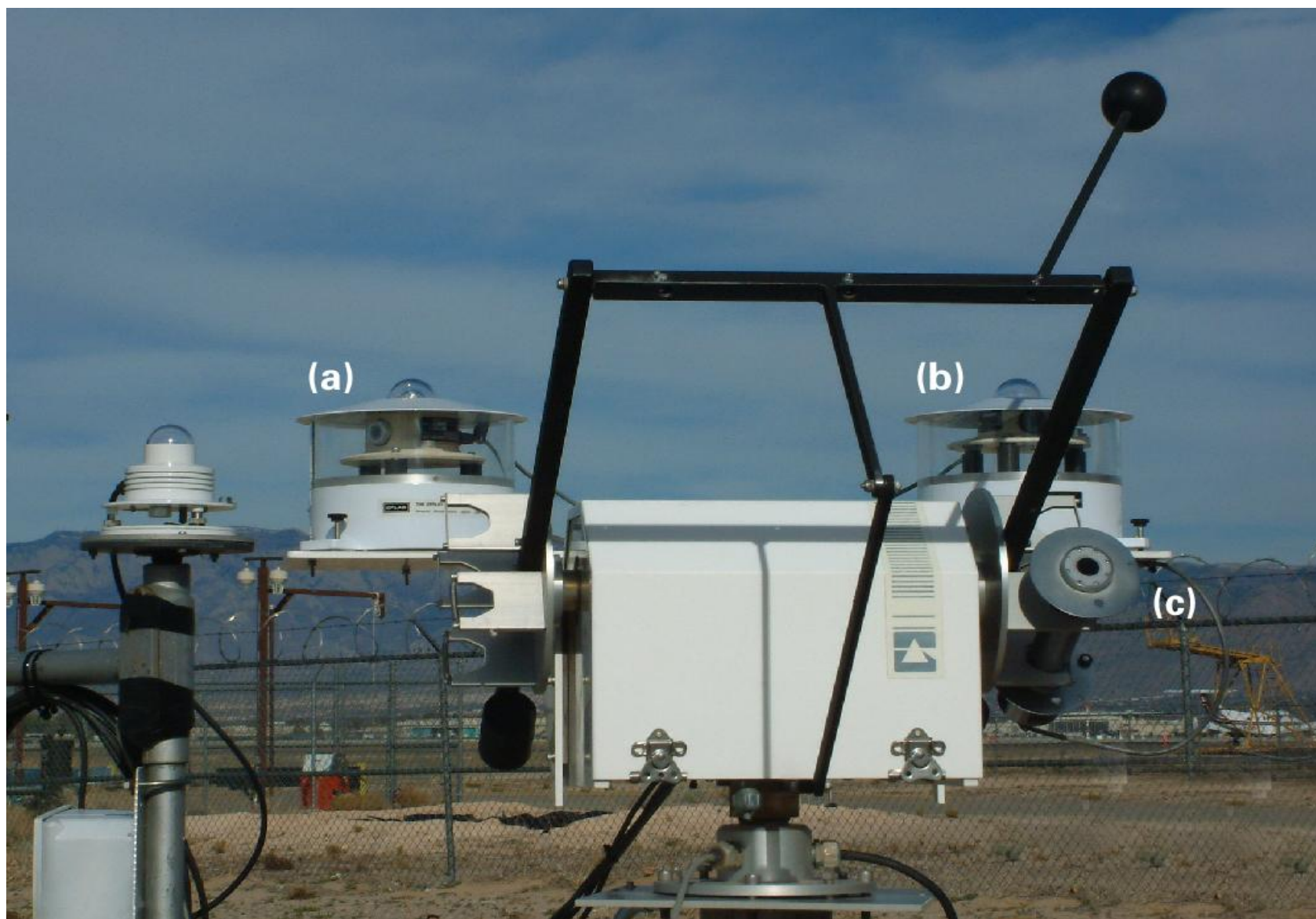
- 数据精度以及均一性问题：比如太阳辐射观测方式的改变是否带来观测资料的均一性问题，不同的仪器提供的观测是否一致？
  - 能否利用相关的间接观测资料，来弥补直接观测资料在时间和空间上的空白？
  - 如何有效利用卫星遥感数据，有效估计地表能量平衡的各分量的长期变化特征？
- 地表能量平衡这些变化对温度变化有什么贡献？**

# 地表入射太阳辐射

# 全球暗化与亮化

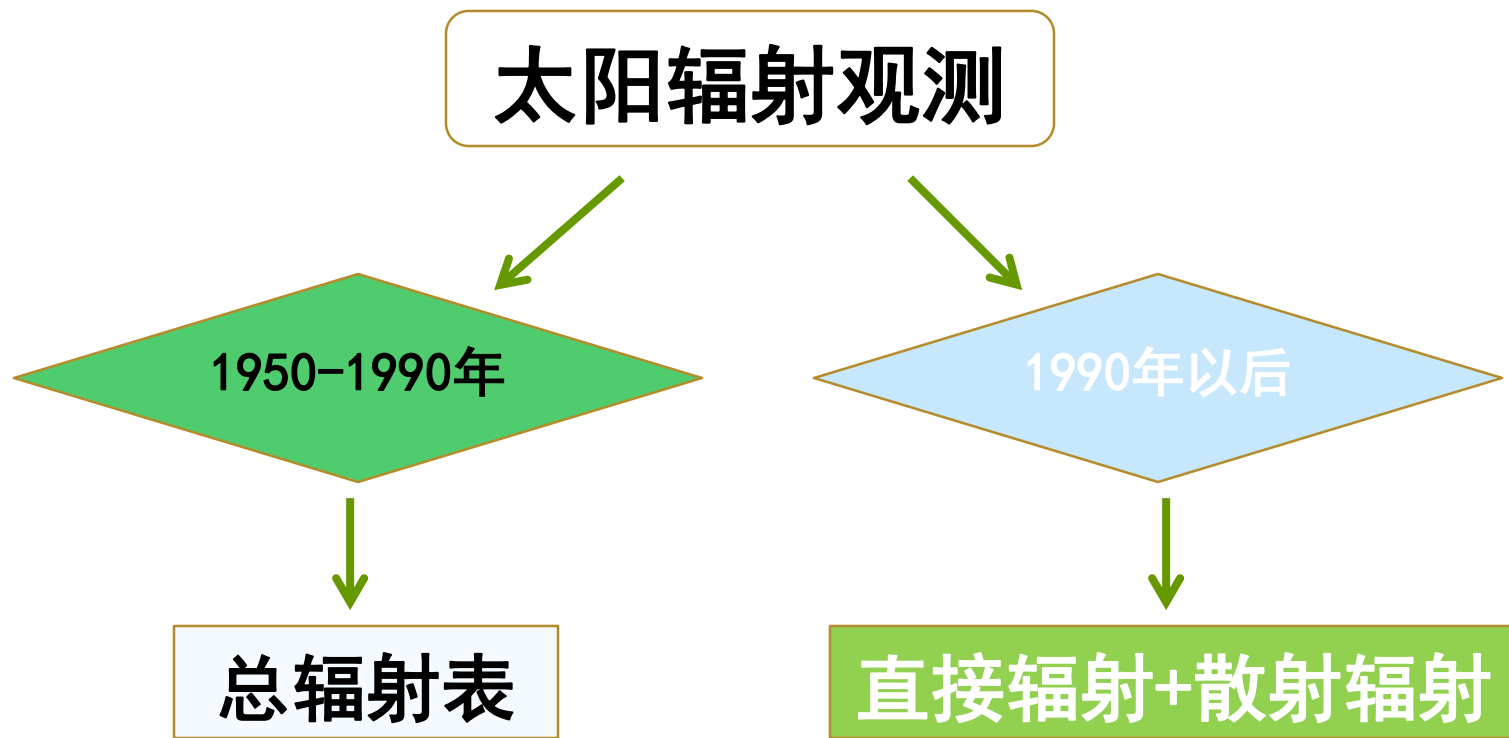
- 观测表明，地表入射太阳辐射在20世纪90年代以前有5-6  $W m^{-2}$  每十年的降低（“全球暗化”），其后太阳辐射以5-6  $W m^{-2}$  每十年的速度增加（“亮化”）。
- 但观测站点太少，并集中在大城市，受到IPCC第四次评估报告的质疑（Kevin Trenberth主导）。
- IPCC第五次评估报告由Martin Wild执笔，他和他的导师（Atsumu Ohmura）是“暗化”和“亮化”的主要倡导者。

# 太阳辐射的观测





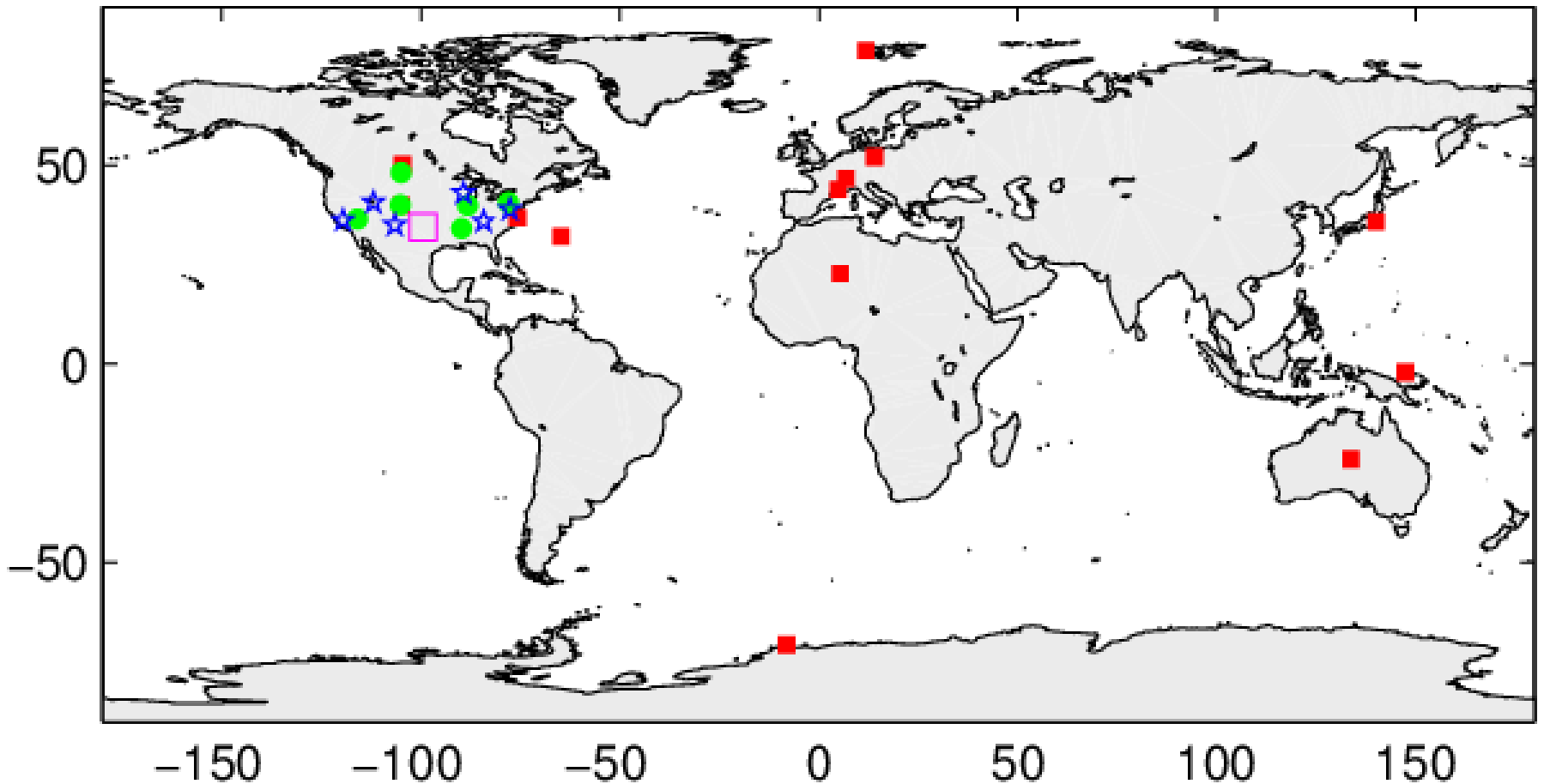
# 太阳辐射数据的长期均一性问题



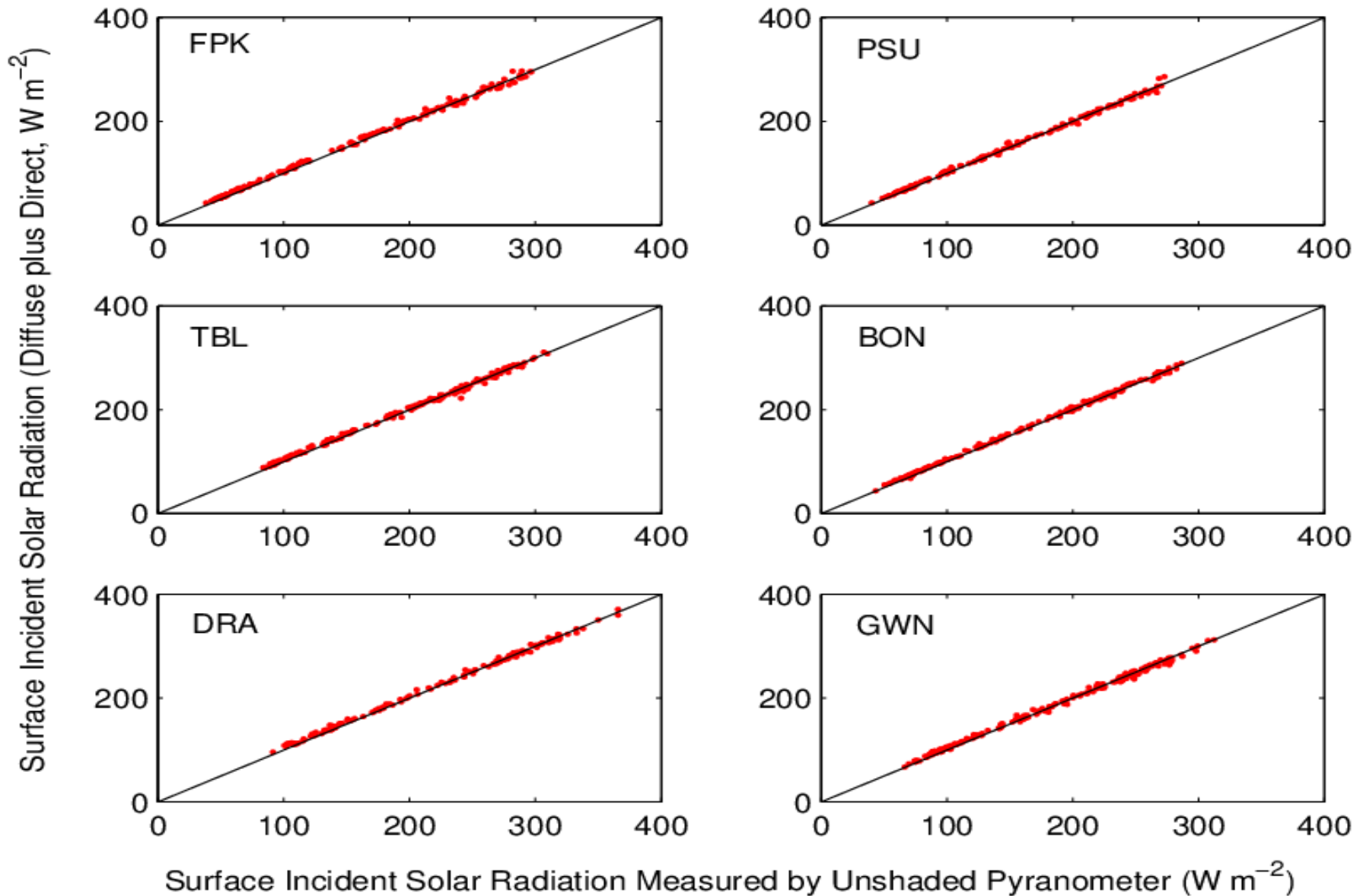
不同的观测方式得到太阳辐射的长期趋势是否一致？

# 全球地表辐射基准站网分布

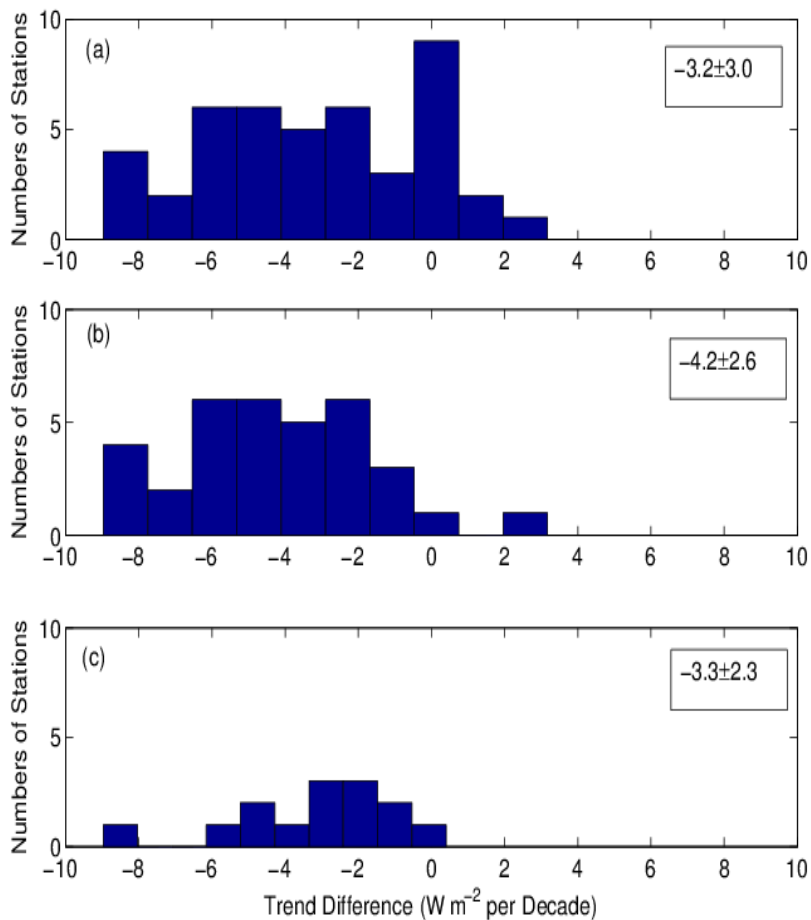
(Wang et al., 2013, JC)



# 两种月平均太阳辐射辐射非常好



# “全球暗化”有一部分来自观测仪器本身



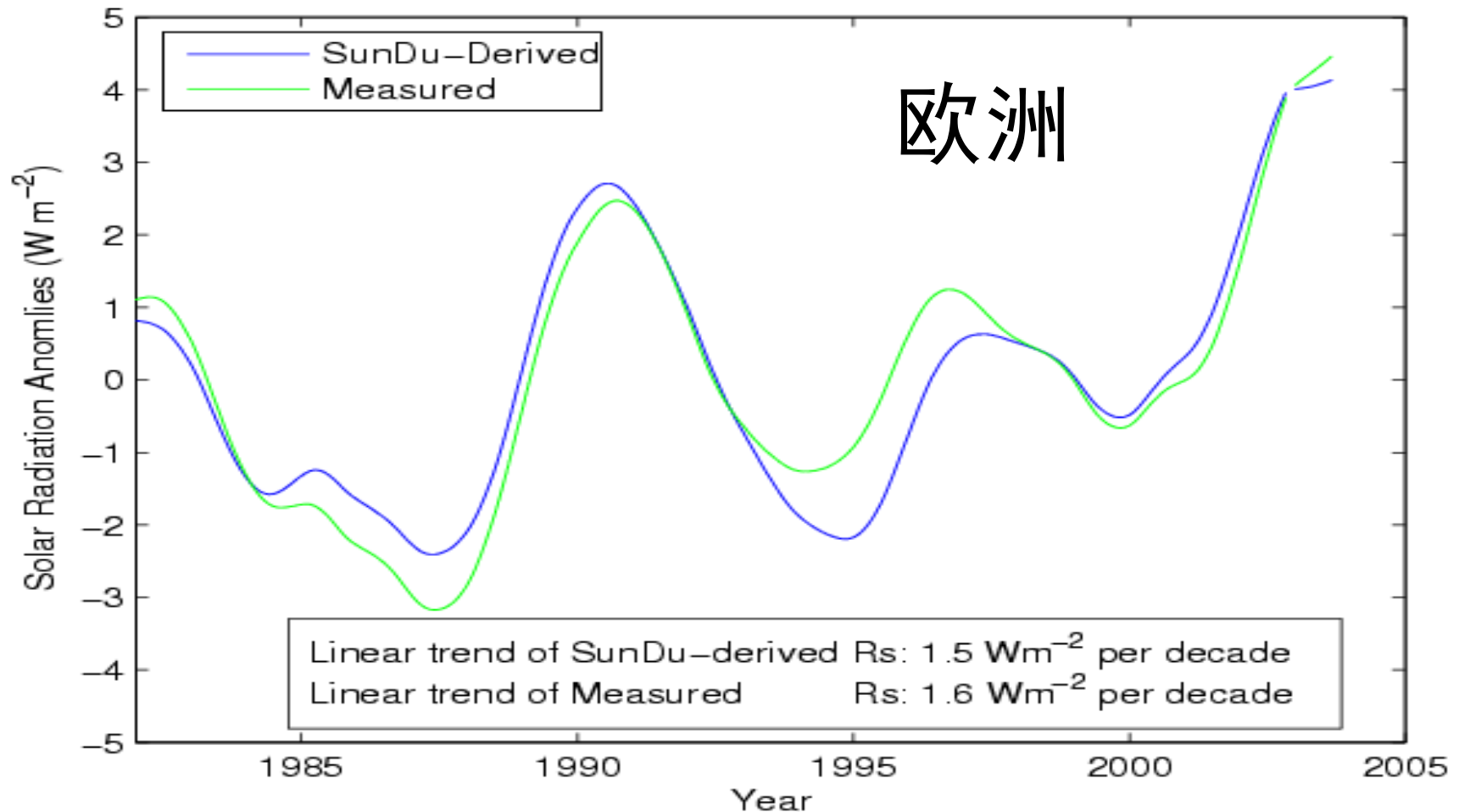
两种观测方式得到太阳辐射长期趋势的差值（总辐射计减去直接辐射计与散射辐射之和）的直方图（单位 $W m^{-2}$  per decade）

BSRN站点同时使用总辐射计和散射计加直射计的方式观测地表入射太阳辐射。

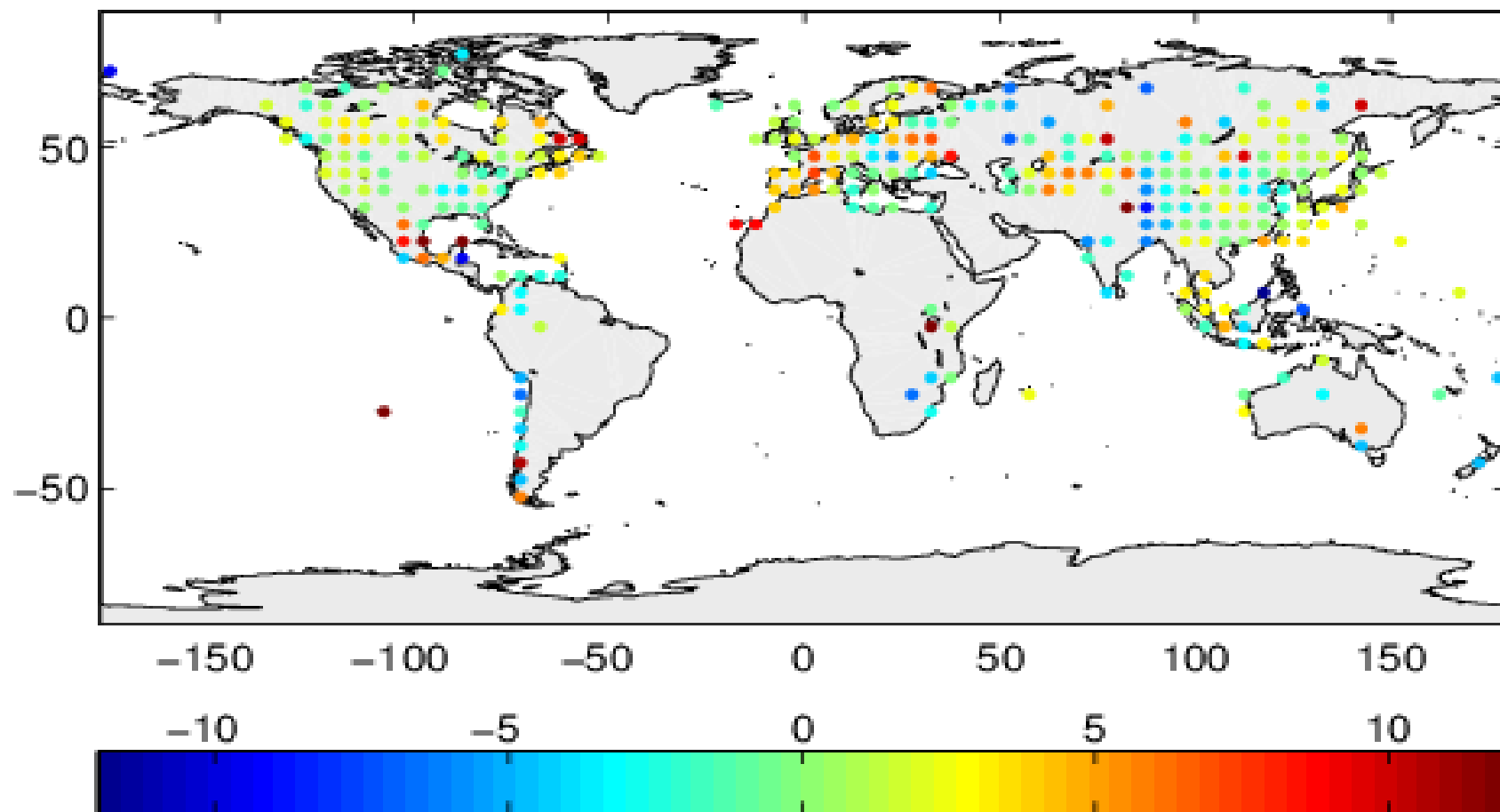
全球BSRN站与美国大气辐射观测计划（ARM）观测站1995到2011年近50个站的资料表明：

总辐射计观测对太阳辐射的长期趋势有每十年 $2-4 W m^{-2}$ 的低估观测。

# 利用日照时数观测可以很好地估计云和气溶胶引起的太阳辐射的长期变化

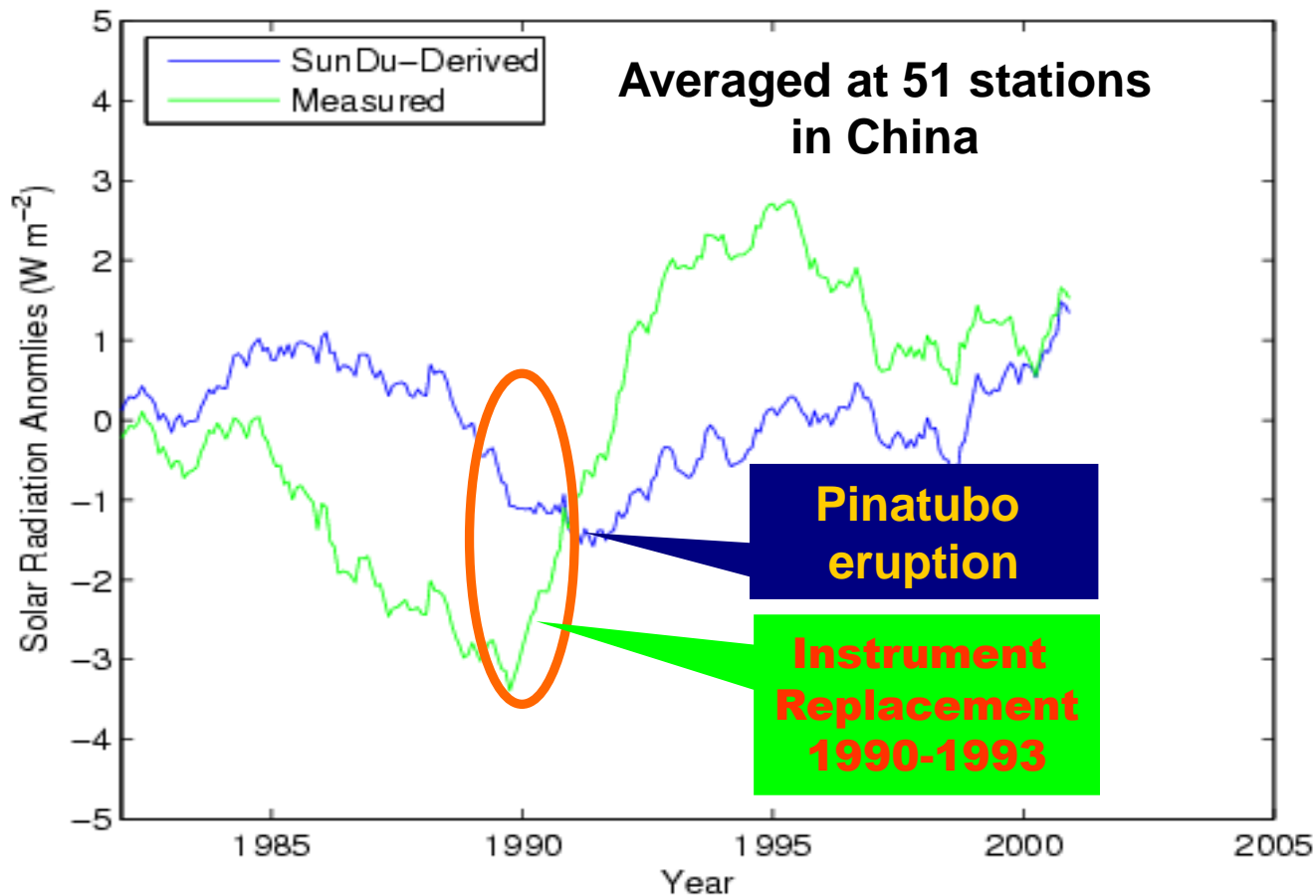


全球陆地上平均地表入射太阳辐射1982年到2008年  
以每十年 $0.87 \text{ W m}^{-2}$  的速度增加。

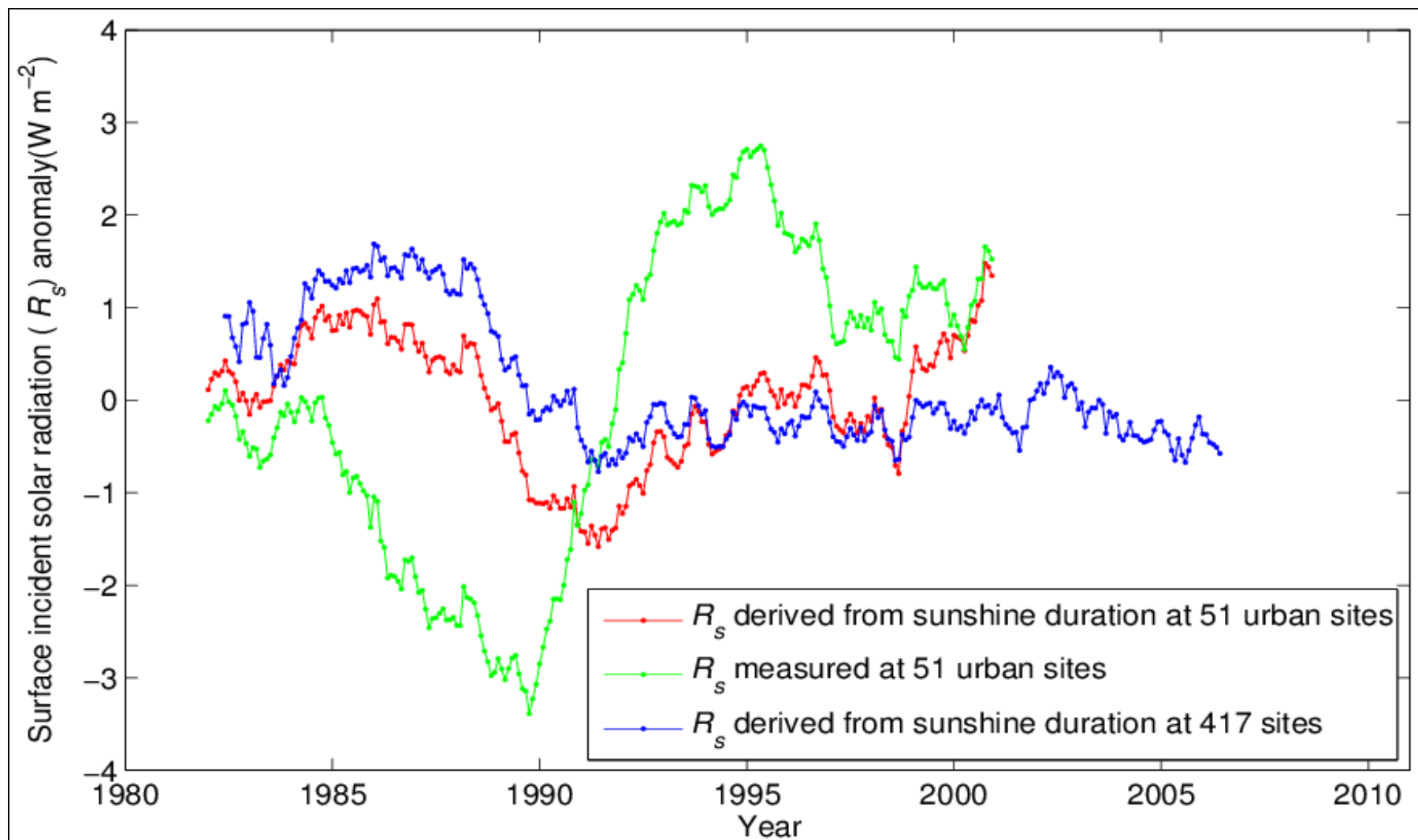


地表入射太阳辐射在1982年到2008年变化趋势（单位： $\text{W m}^{-2}$  per decade）

# 中国区域观测得到太阳辐射在1990年代初期的突然亮化与仪器更换有关



# 中国区域太阳辐射直接观测有明显的城市偏差



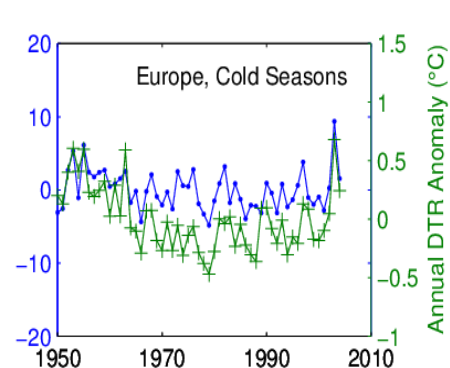
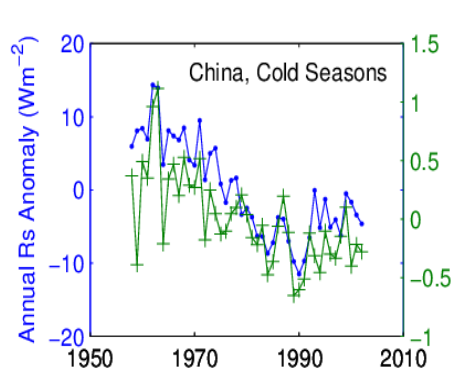
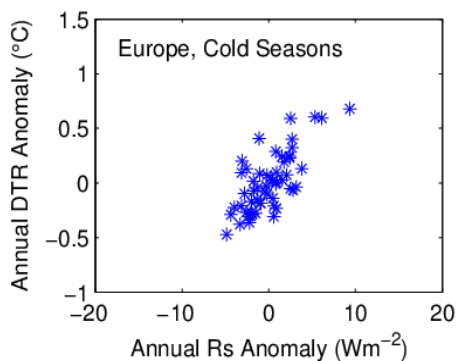
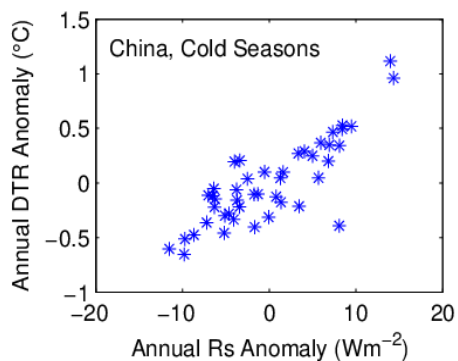
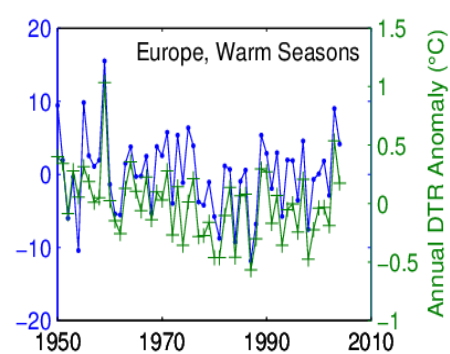
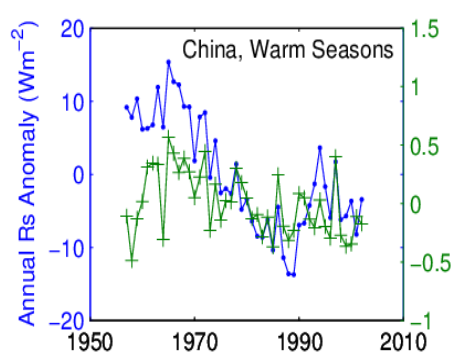
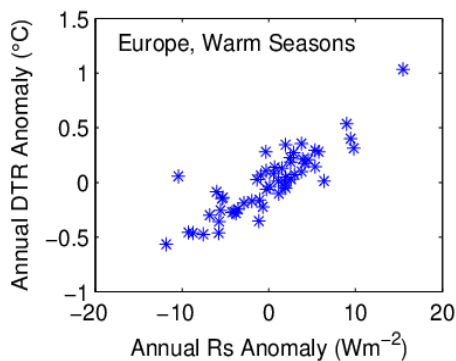
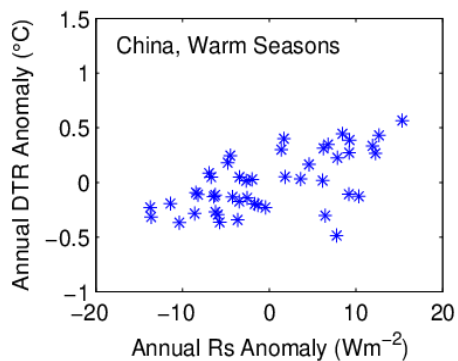


# 利用温度日较差重建地表太阳辐射

(Wang and Dickinson, PNAS, 2013)

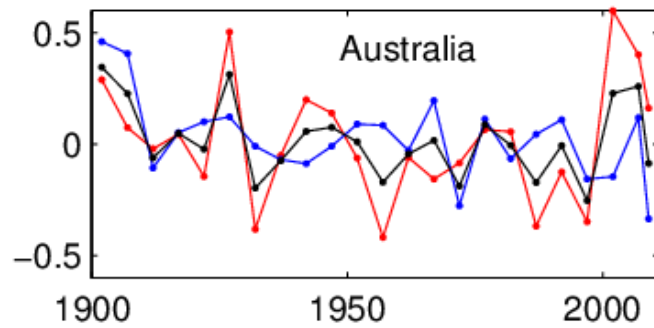
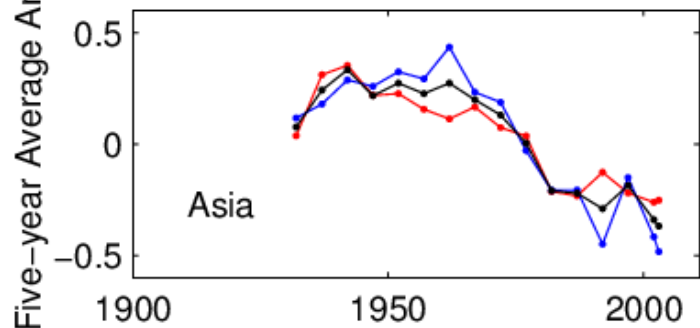
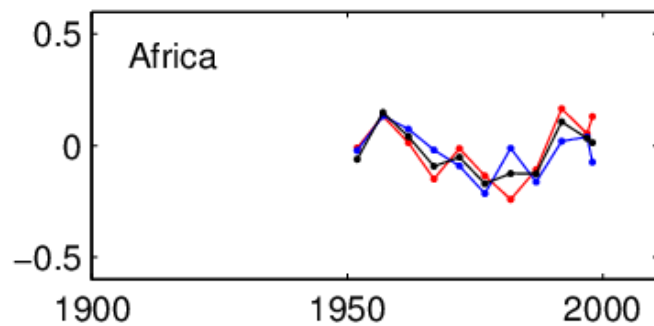
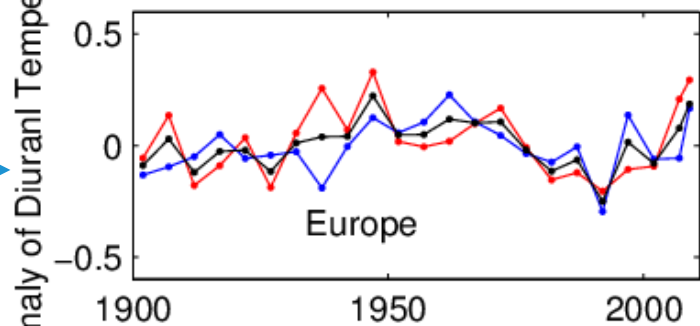
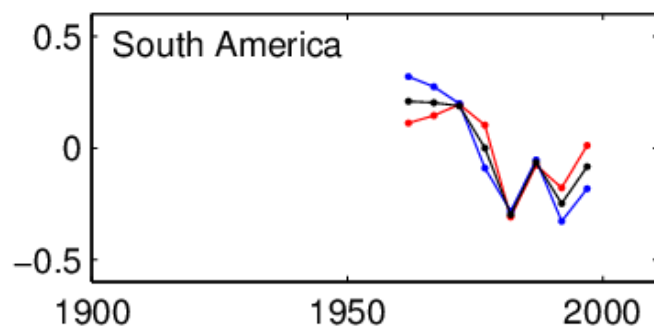
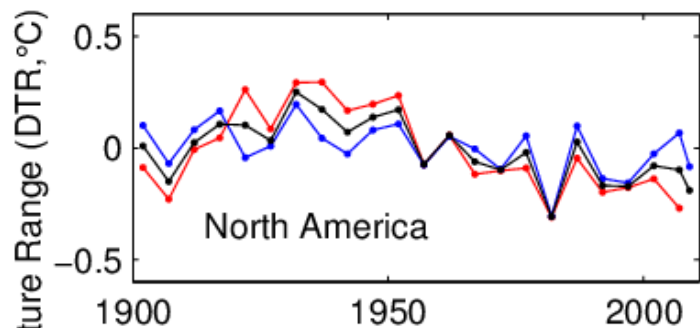
- 因为长波辐射冷却的作用，陆地地表气温一般在日出前达到最低温度（ $T_{min}$ ）。
- 日出后，地表吸收太阳辐射 $R_s$ ，地表温度高于近地面气温，产生湍流，通过感热通量加热大气，因此地表气温在午后2小时左右达到最大值（ $T_{max}$ ）。
- 因此日平均太阳辐射被认为与温度日较差（ $DTR=T_{max}-T_{min}$ ）相关。
- 它们之间的关系决定于地表吸收的太阳辐射有多少转化成了感热通量。

# 区域平均太阳辐射与温度日较差 (Wang and Dickinson, PNAS, 2013)



# 过去百年陆地上温度日较差

黑线：年平均 红线：暖季（5-10月） 蓝线：冷季（11-4月）



# 地表太阳辐射变化对气温年变化的贡献

Table 1. The impact of  $R_s$  on daily mean air temperature ( $T_a$ ) during three periods, 1900–2010, 1985–2010, and 1940–1984 (in °C per 100 y)

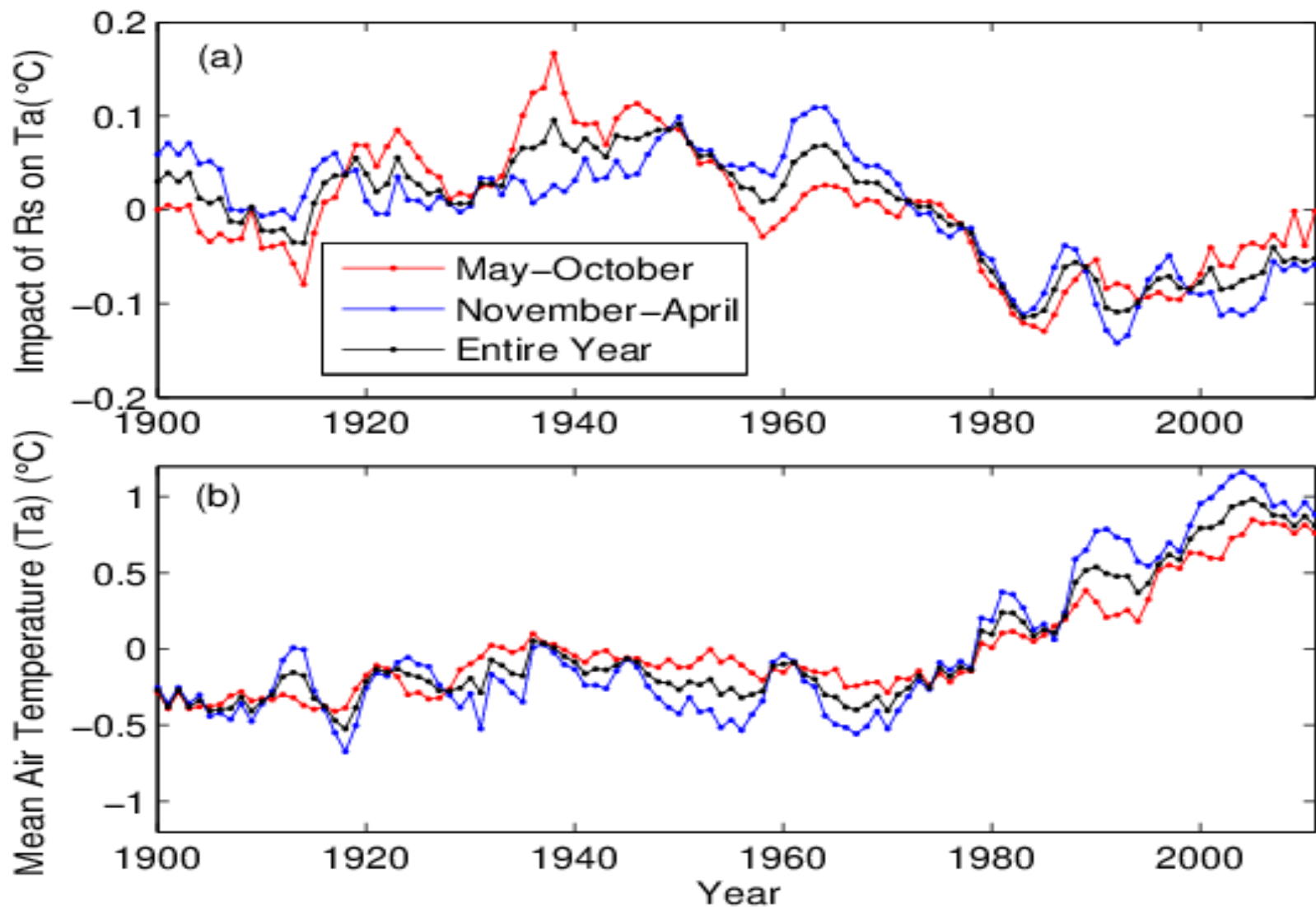
Time periods	Global land	North America	South America	Europe	Africa	Asia	Australia
Yearly							
1900–2010 <sup>a</sup>	–0.11*	–0.11*	–0.68*	0.01	–0.04	–0.50*	–0.084
1985–2010 <sup>b</sup>	0.07	–0.21	–0.23	0.46*	0.34	–0.57*	0.80
1940–1984	–0.36*	–0.46*	–1.04*	–0.24*	–0.29*	–0.53*	–0.08
Warm seasons							
1900–2010 <sup>a</sup>	–0.11*	–0.15*	–0.47	–0.01	0.03	–0.43*	–0.06
1985–2010 <sup>b</sup>	0.19	–0.31	–0.03	0.75*	1.10*	–0.22	1.96*
1940–1984	–0.45*	–0.62*	–0.82	–0.29*	–0.43*	–0.54*	–0.08
Cold seasons							
1900–2010 <sup>a</sup>	–0.12*	–0.07	–0.82*	0.03	–0.14	–0.52*	–0.09
1985–2010 <sup>b</sup>	–0.09	–0.02	–0.28	0.27	0.49	–0.50	–0.41
1940–1984	–0.29*	–0.22	–1.58*	–0.20*	–0.28	–0.55*	0.03

Negative values indicate that  $R_s$  reduced the rate of warming caused by the elevated GHG, and positive values mean that  $R_s$  amplified the warming rate by GHG. We also divide the data into boreal warm seasons (May to October) and cold seasons (November to April). The asterisk represents impact of  $R_s$  is statistically significant (i.e., pass the Student's  $t$  confidence test at  $\alpha = 0.05$ ).

<sup>a</sup>Time periods for different regions are different and may cover only a fraction of 1900–2010 (Fig. 5).

<sup>b</sup>Time periods for different regions are different and may cover only a fraction of 1985–2010 (Fig. 5).

# 全球增温停滞：现象与原因



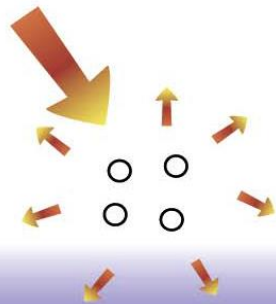
# 气溶胶

# 气溶胶的变化及其辐射效应是目前气候变化研究中的最大的不确定性因素

## Aerosol-radiation interactions

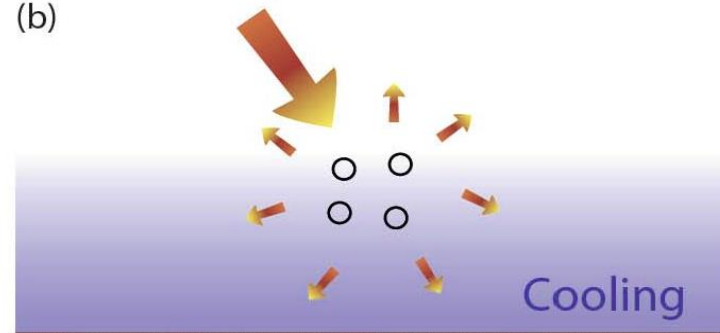
### Scattering aerosols

(a)



Aerosols scatter solar radiation. Less solar radiation reaches the surface, which leads to a localised cooling.

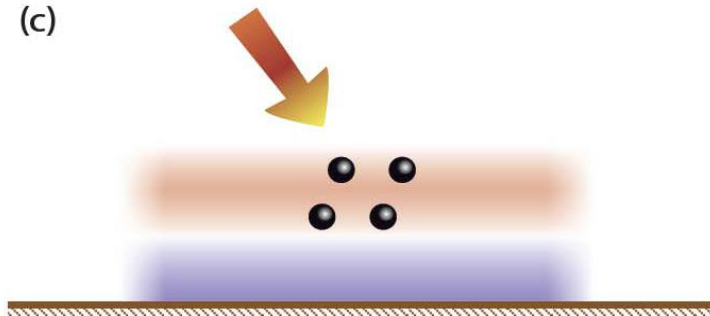
(b)



The atmospheric circulation and mixing processes spread the cooling regionally and in the vertical.

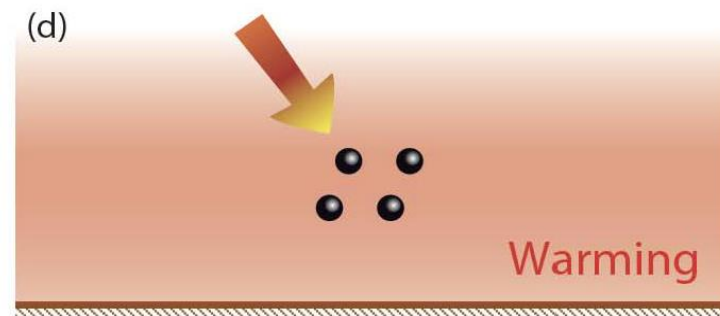
### Absorbing aerosols

(c)



Aerosols absorb solar radiation. This heats the aerosol layer but the surface, which receives less solar radiation, can cool locally.

(d)



At the larger scale there is a net warming of the surface and atmosphere because the atmospheric circulation and mixing processes redistribute the thermal energy.

# 利用能见度估计 全球陆地上空大气气溶胶光学厚度



**Clear Sky Visibility Has Decreased over Land Globally from 1973 to 2007**  
Kaicun Wang, *et al.*  
*Science* 323, 1468 (2009);  
DOI: 10.1126/science.1167549



## Clear Sky Visibility Has Decreased over Land Globally from 1973 to 2007

Kaicun Wang,<sup>1\*</sup> Robert E. Dickinson,<sup>2</sup> Shunlin Liang<sup>1</sup>

Visibility in the clear sky is reduced by the presence of aerosols, whose types and concentrations have a large impact on the amount of solar radiation that reaches Earth's surface. Here we establish a global climatology of inverse visibilities over land from 1973 to 2007 and interpret it in terms of changes in aerosol optical depth and the consequent impacts on incident solar radiation. The aerosol contribution to "global dimming," first reported in terms of strong decreases in measured incident solar radiation up to the mid-1980s, has monotonically increased over the period analyzed. Since that time, visibility has increased over Europe, consistent with reported European "brightening," but has decreased substantially over south and east Asia, South America, Australia, and Africa, resulting in net global dimming over land.

Uncertainty about how much the concentration of atmospheric aerosols has increased over the past century and its impact on the global radiation balance have been major obstacles to establishing how observed changes of climate are related to changes in greenhouse gas concentrations. Some long-period observational constraints on aerosols are provided by measurement of solar radiation incident at the surface (1) and by estimation of emissions by fossil fuel combustion (2). The former can be equally or more greatly affected by changes of cloudiness (3), and the latter can be used to estimate changes of limited aerosol types (2). Much better estimates of global aerosol impacts can be made over the past decade from both surface and satellite measurements of aerosol optical depth (AOD) (4, 5). For a given vertical profile of aerosols, the meteorological visibility inverse (Vil) is directly proportional to AOD. Thus, we can use these recent measure-

ments of AOD to evaluate the accuracy of Vil in terms of its mean and spatial variability. This evaluation establishes the Vil climatology as a data set that characterizes the spatial and temporal variability of over-land aerosols for the past several decades.

We calculated Vil in  $\text{km}^{-1}$  from the National Climatic Data Center (NCDC) Global Summary of Day (GSOD) database collected from about 3250 meteorological stations from 1973 to 2007. It is multiplied by a scaling factor of 1.0 km, as inferred from rules described in (6). This index is used as an estimate of AOD for a particular aerosol profile, and has other uncertainties described in (6). However, its evaluation against other more recent and more direct data sets shows that it estimates AOD with an accuracy comparable to that of the other measures (6) and thus can be used to discuss the effects of aerosols on the incidence of solar radiation.

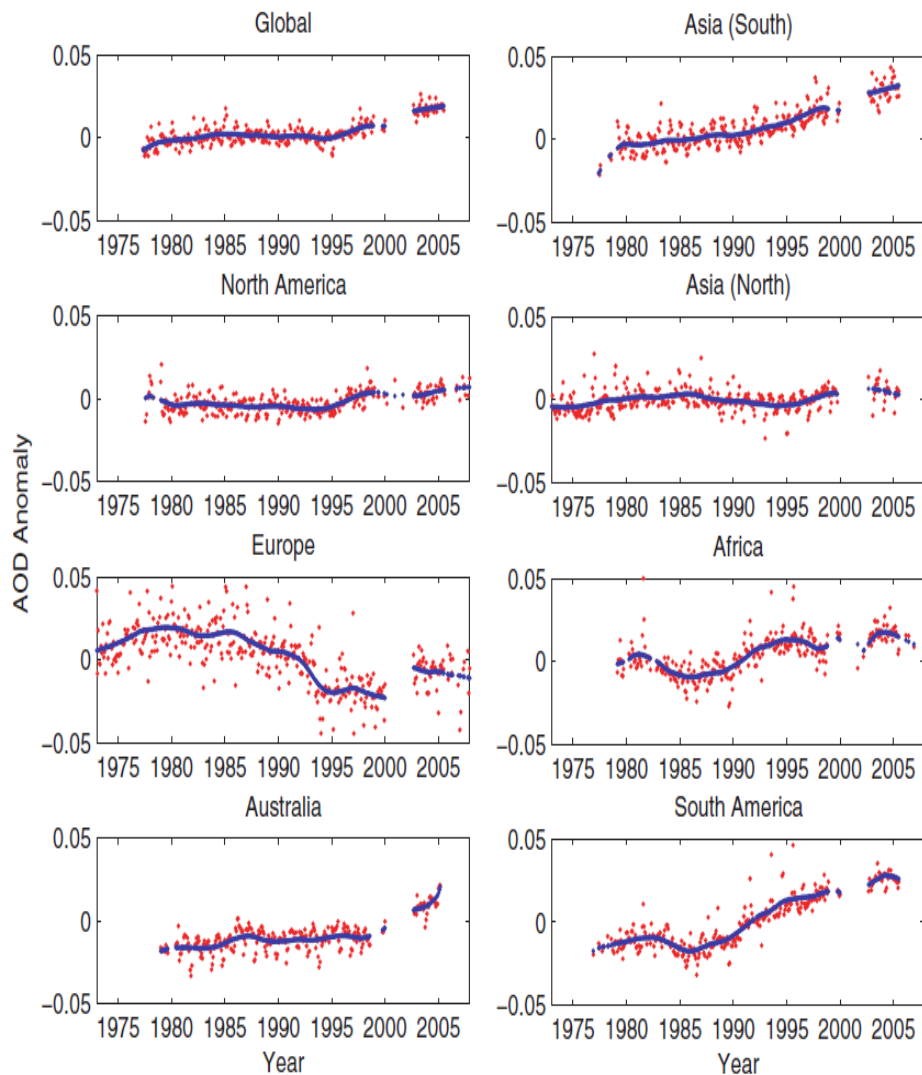
The geographic long-term variation of this AOD measure is determined by aggregating the meteorological station data into continental regions where such data are available, removing time means, and calculating the area-weighted monthly anomaly values for regions where data are available for more than 80% of the stations [see

(6) for explanation of the gap; see fig. S7 for domains). Aerosols increased on average over all continental regions between 1979 and 2006, with the exception of Europe (Fig. 1). In particular they increased from 1979 over Australia and south Asia (including India and China), decreased over South America and Africa from 1979 to about 1985, and then increased and were relatively unchanged over north Asia (Siberia).

The large increases of Asian AODs likely were consequences of large increases in industrial activities and are consistent with long-term observations of incident solar radiation and cloud cover in India (7) and China (8). The European decrease are consistent with numerous past studies based on long-term measurements of aerosols, solar radiation, and clouds (9-11), which are consistent with changes in emissions of aerosol precursors, SO<sub>2</sub> (12, 13), black carbon (14), and organic carbon (14, 15).

The variability of measured changes between stations from 1973 to 2007 is summarized in terms of linear trends for the period 1973 to 2007. Figure 2 shows the spatial distribution of the 58% of the stations that have magnitudes of their trends greater than  $0.0015 \text{ year}^{-1}$ —that is, 50% larger than the global area-weight average linear trend of  $0.001 \text{ year}^{-1}$ . This change in AOD is not the same everywhere; AODs substantially declined in Europe after peaking in the 1980s. These changes vary widely from location to location (Fig. 2). Overall, the largest increases of AOD have been in Asia, and these increases have accelerated over the past decade, producing the rapid global increase over this period.

Aerosols reduce solar radiation at Earth's surface by upward reflection and absorption. The energy lost in this manner either escapes to space or heats the air. Aerosols can further affect surface radiation by modifying cloud cover and other cloud properties. The long-term trend in over-land Vil AOD that we report is consistent with the long-term variation in incident solar radiation in China, India, and Europe (7-11). Wild *et al.* (1) documented that solar radiation



<sup>1</sup>Department of Geography, University of Maryland, College Park, MD 20742, USA. <sup>2</sup>Department of Geological Sciences, University of Texas, Austin, TX 78712, USA.

\*To whom correspondence should be addressed. E-mail: kcwang@umd.edu



# IPCC 第五次评价报告的引用和评价

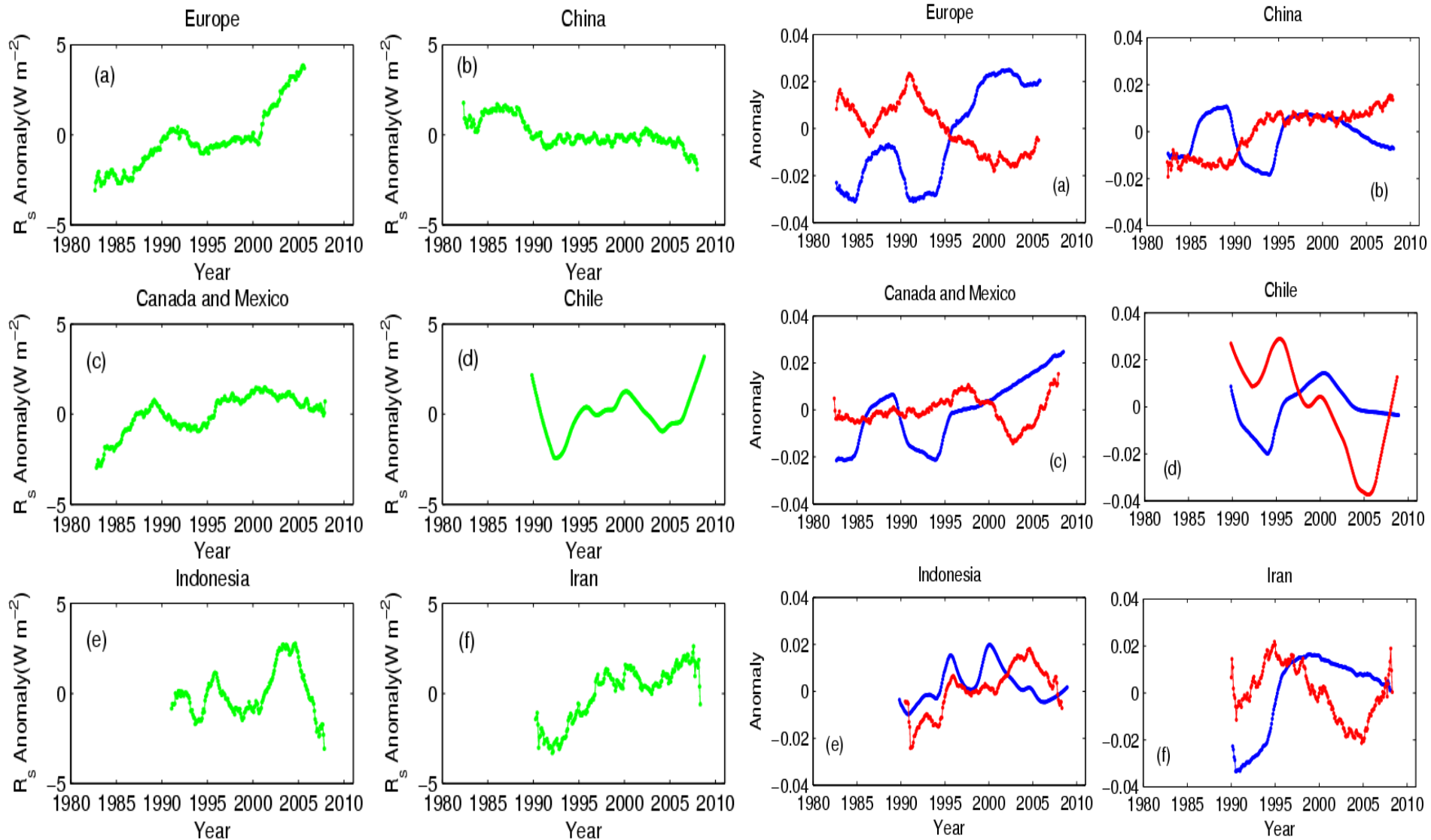
AOD sun photometer measurements starting in 1986 at two stations in northern Germany corroborate the long-term decline of AOD in Europe (Ruckstuhl et al., 2008). Ground-based, cloud-screened solar broadband radiometer measurements provide longer time-records than spectrally selective sun-photometer data, but are less specific for aerosol retrieval. Multi-decadal records over Japan (Kudo et al., 2011) indicate an AOD increase until the mid-1980s, followed by an AOD decrease until the late 1990s and almost constant AOD in the 2000s. Similar broad-band solar radiative flux multi-decadal trends have been observed for urban-industrial regions of Europe and North America (Wild et al., 2005), and were linked to successful measures to reduce sulphate emissions since the mid-1980s (Section 2.3). An indirect method to estimate AOD is offered by ground-based visibility observations. These data are more ambiguous to interpret, but records go further back in time than broadband, sun photometer and satellite data. A multi-regional analysis for 1973-2007 (Wang et al., 2009a) shows that prior to the 1990s visibility-derived AOD was relatively constant in most regions analysed (except for positive trends in southern Asia), but after 1990 positive AOD trends were observed over Asia, and parts of South America, Australia and Africa, and mostly negative AOD trends were found over Europe. In North America, a small step-wise decrease of visibility after 1993 was likely related to methodological changes (Wang et al., 2012f).

利用地基能见度观测可以间接地估计气溶胶光学厚度AOD。AOD与能见度的关系比较复杂，但能见度资料要比宽波段和分光辐射观测以及卫星遥感数据时间跨度要长。1973-2007年多区域的分析表明（Wang et al., 2009a）1990年代以前 AOD除亚洲地区增加外，其它区域AOD近乎不变。1990年以后，亚洲、南美洲的一部分，澳大利亚和非洲AOD增加，欧洲地区降低。1993年以后北美洲的能见度有所降低，这可能是与能见度的观测方式改变有关(Wang et al., 2012f)。

# 气溶胶的变化是影响地表太阳辐射的长期变化的重要因子

(Wang et al., ACP, 2012)

绿线：太阳辐射； 红线：总云量的负数； 蓝线：气溶胶光学厚度的负数

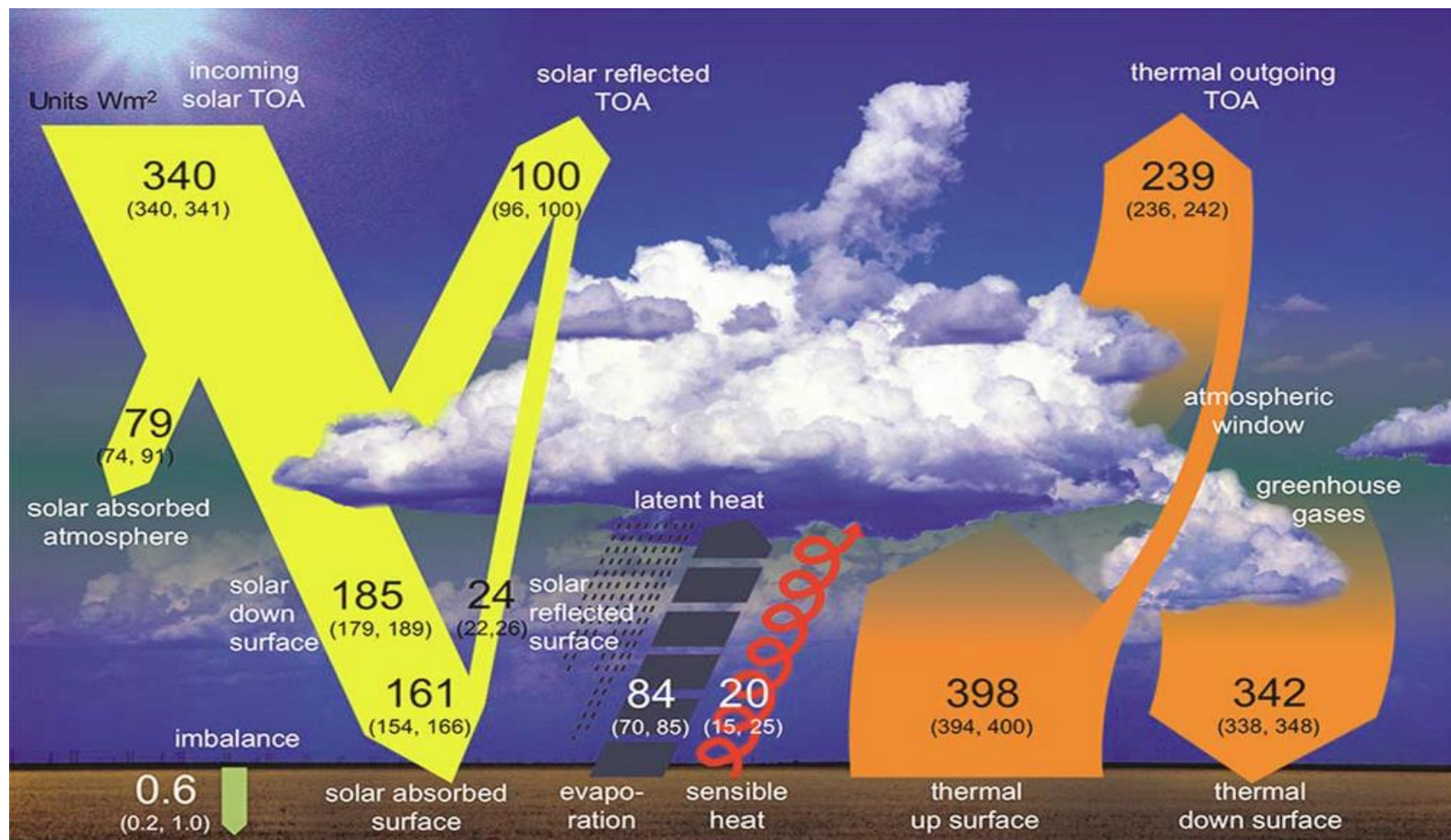


# 大气向下长波辐射

# 目前对大气向下长波辐射的全球平均值有较大争议

- 大气长波辐射是地表辐射平衡四个分量中不确定性最大的一个。
- Kevin Trenberth认为全球平均值为 $333 \text{ W m}^{-2}$ ，Graeme L. Stephens认为在 $344\text{-}350 \text{ W m}^{-2}$ 之间（IPCC 第五次评估报告的主导者之一），并被写入IPCC 第五次评估报告初稿。
- 我们认为为 $342 \text{ W m}^{-2}$ ，这一结果被IPCC 第五次评估报告修改稿认可。

# 全球能量平衡



# 产生争议的原因

- 缺乏大气向下长波辐射的长期连续观测。
- 全球平均大气长波向下辐射的估计主要来自卫星遥感反演，再分析资料和全球气候模式模拟。这些资料均有可能有较大的误差。
- 地基稀疏站点的观测资料被用来验证卫星，再分析和模式资料，去除系统偏差，从而得到全球平均值的估计。
- 但一个重要问题长期被忽视：观测资料的精度如何？有无偏差？

# 大气 向下长波辐射观测



# 美国通量网所用辐射表





A new moored buoy array in the historically data-sparse Indian Ocean provides measurements to advance monsoon research and forecasting.



**The Ocean Research Vessel *Sagar Kanya*, operated by the Indian Ministry of Earth Sciences, deploys a NOAA ATLAS mooring in the Indian Ocean. (Photo: M. Craig, NOAA)**

# 长波辐射表校准方法不统一。2007年以前只有实验室校准，缺乏可靠的野外校准方法

- 两种校准长波辐射表方法:

$$L_d = \frac{V}{A} + \sigma T_B^4 - B\sigma(T_D^4 - T_B^4)$$

$$L_d = \frac{V}{C} \left(1 + k_1 \sigma T_B^3\right) + k_2 \sigma T_B^4 - k_3 \sigma (T_D^4 - T_B^4)$$

- 2007年世界辐射中心建立了世界长波辐射标准器组，可以用于对长波辐射表进行野外校准。在此之前，长波辐射表的校准均在实验室进行，很难估计环境变化和太阳直接辐射对观测结果的影响。

# BSRN

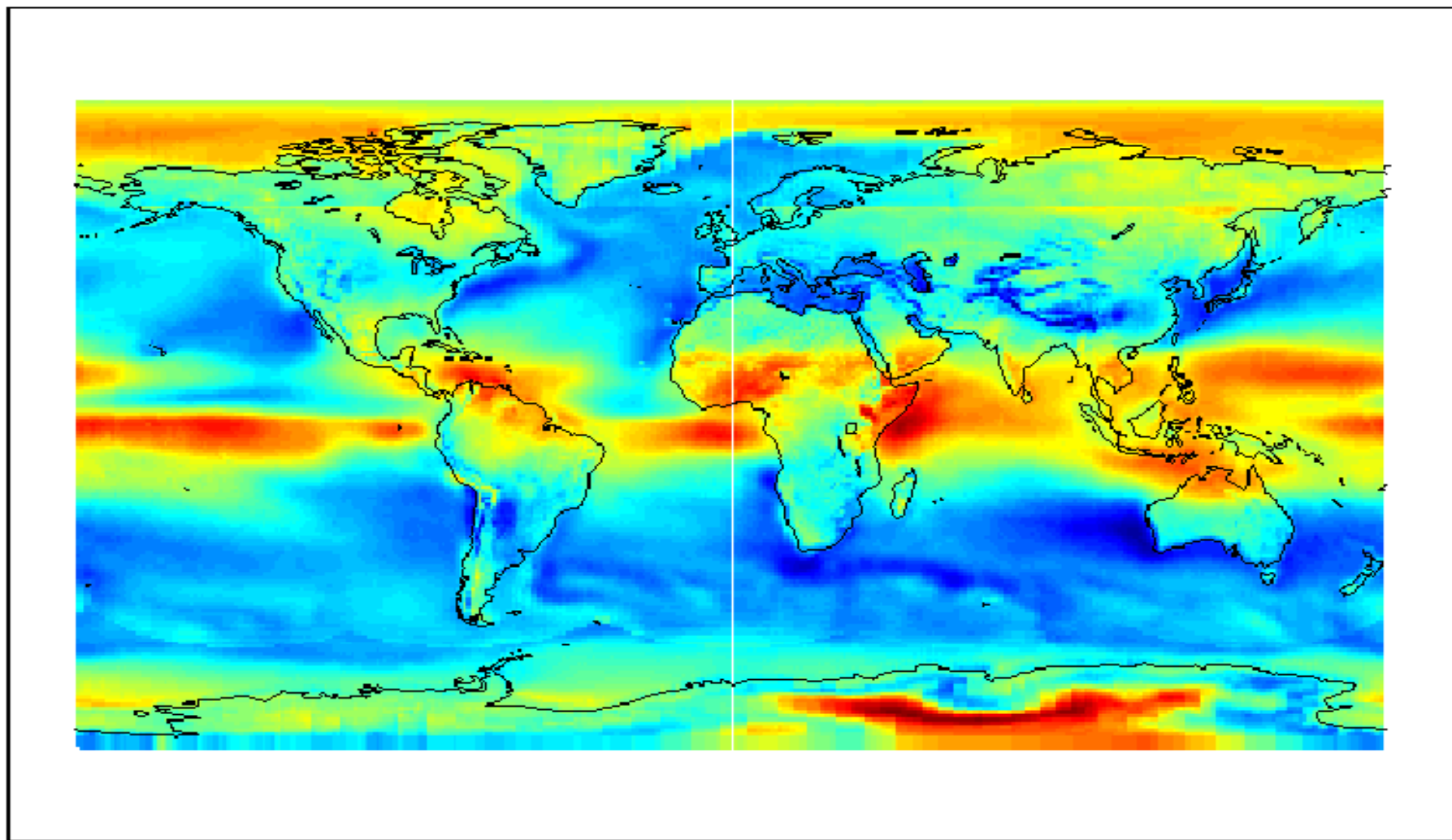
Products	Bias	Standard deviation	Correlation coefficient	Global average of $L_d$ ( $\text{W m}^{-2}$ )
GEWEX-SRB	2.53 (9.63)	9.95	0.96 (0.72)	308.20
CERES SYN	0.14 (9.29)	7.22	0.98 (0.77)	307.15
CSFR	-0.19 (12.67)	8.38	0.97 (0.80)	305.23
ERA-Interim	-2.31 (9.31)	7.93	0.97 (0.80)	304.23
MERRA	-14.51 (9.47)	8.47	0.97 (0.78)	295.07

## Buoy Measurements in Tropical Oceans

Products	Bias	Standard Deviation	Correlation Coefficient	Global Average of $L_d$ ( $\text{W m}^{-2}$ )
GEWEX-SRB	-3.13 (4.14)	4.37	0.89	308.20
CERES SYN	-4.17 (5.76)	3.79	0.88	307.15
CSFR	-2.79 (9.16)	5.68	0.77	305.23
ERA-Interim	-3.71 (5.45)	4.59	0.90	304.23
MERRA	-11.65 (7.93)	5.45	0.85	295.07

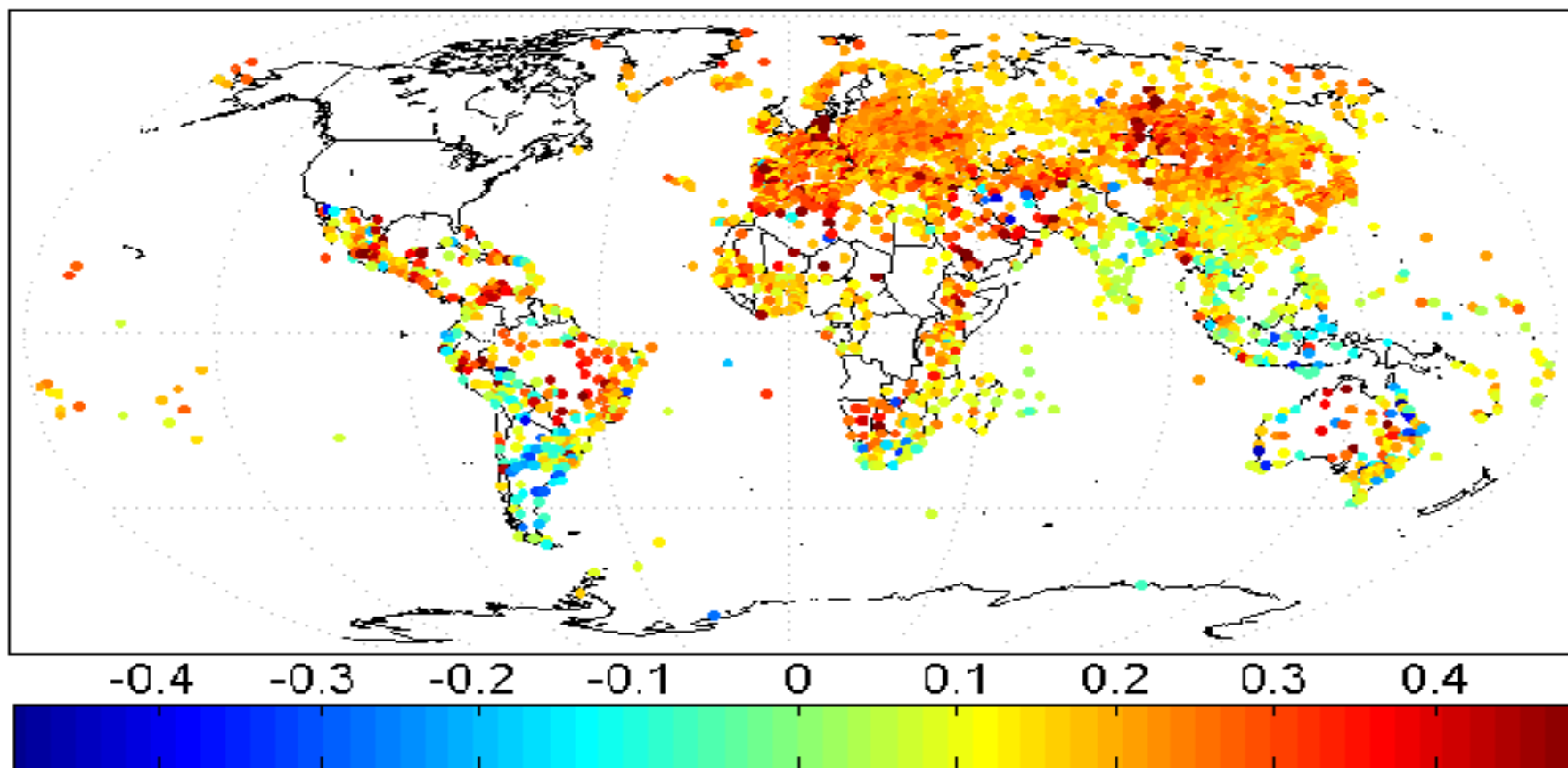
云是影响大气长波辐射估计的重要因素

图为全球观测与模拟云覆盖之差 (MERRA-CERES)



利用1973-2008年间全球3800个气象站的地面观测计算大气向下长波辐射，发现它以每十年  $2.2 \text{ Wm}^{-2}$  的速度增加 (Wang and Liang, JGR, 2009)

Trend in Downward Longwave Radiation ( $\text{W m}^{-2} \text{ ya}^{-1}$ )



# IPCC 第五次评价报告的引用

## 2.3.3.2 *Surface Thermal and Net Radiation*

Thermal radiation, also known as longwave, terrestrial or far-infrared radiation is sensitive to changes in atmospheric greenhouse gases, temperature and humidity. Long-term measurements of the thermal surface components as well as surface net radiation are available at far fewer sites than SSR. Downward thermal radiation observations started to become available during the early 1990s at a limited number of globally distributed terrestrial sites. From these records, Wild et al. (2008) determined an overall increase of  $2.6 \text{ W m}^{-2}$  per decade over the 1990s, in line with model projections and the expectations of an increasing greenhouse effect. Wang and Liang (2009) inferred an increase in downward thermal radiation of  $2.2 \text{ W m}^{-2}$  per decade over the period 1973–2008 from globally available terrestrial observations of temperature, humidity and cloud fraction. Prata (2008) estimated a slightly lower increase of  $1.7 \text{ W m}^{-2}$  per decade for clear sky conditions over the earlier period 1964–1990, based on observed temperature and humidity profiles from globally distributed land-based radiosonde stations and radiative transfer calculations. Philipona et al. (2004; Philipona et al., 2005) and Wacker et al. (2011) noted increasing downward thermal fluxes recorded in the Swiss Alpine Surface Radiation Budget (ASRB) network since the mid-1990s, corroborating an increasing greenhouse effect. For mainland Europe, Philipona et al. (2009) estimated an increase of downward thermal radiation of  $2.4\text{--}2.7 \text{ W m}^{-2}$  per decade for the period 1981–2005.

**Wang and Liang (2009)利用全球可以利用的地基温度、湿度和云量观测计算得到1973-2008年间全球平均大气向下辐射以 $2.2 \text{ W m}^{-2}$  per decade的速度增加。**

# 陆地蒸散

# 全球陆地蒸散的综述

## A REVIEW OF GLOBAL TERRESTRIAL EVAPOTRANSPIRATION: OBSERVATION, MODELING, CLIMATOLOGY, AND CLIMATIC VARIABILITY

Kaicun Wang<sup>1</sup> and Robert E. Dickinson<sup>2</sup>

Received 6 September 2011; revised 20 March 2012; accepted 21 March 2012; published 24 May 2012.

[1] This review surveys the basic theories, observational methods, satellite algorithms, and land surface models for terrestrial evapotranspiration,  $E$  (or  $\lambda E$ , i.e., latent heat flux), including a long-term variability and trends perspective. The basic theories used to estimate  $E$  are the Monin-Obukhov similarity theory (MOST), the Bowen ratio method, and the Penman-Monteith equation. The latter two theoretical expressions combine MOST with surface energy balance. Estimates of  $E$  can differ substantially between these three approaches because of their use of different input data.

**Citation:** Wang, K., and R. E. Dickinson (2012), A review of global terrestrial evapotranspiration: Observation, modeling, climatology, and climatic variability, *Rev. Geophys.*, 50, RG2005, doi:10.1029/2011RG000373.

### 1. INTRODUCTION

[2] Terrestrial evapotranspiration,  $E$ , is the water transferred from the land surface to the atmosphere. This water exchange usually involves a phase change of water from liquid (or ice) to gas, which absorbs energy and cools the land surface. The latent heat accompanying  $E$  is  $\lambda E$ , where  $\lambda$  is the latent heat of vaporization. This review uses  $E$  or  $\lambda E$  interchangeably depending on whether water or energy flux is the primary consideration. These terms are required by short-term numerical weather prediction models and longer-term climate simulations and for diagnoses of climate change. In such models,  $E$  is generally parameterized as a sum of soil

Surface and satellite-based measurement systems can provide accurate estimates of diurnal, daily, and annual variability of  $E$ . But their estimation of longer time variability is largely not established. A reasonable estimate of  $E$  as a global mean can be obtained from a surface water budget method, but its regional distribution is still rather uncertain. Current land surface models provide widely different ratios of the transpiration by vegetation to total  $E$ . This source of uncertainty therefore limits the capability of models to provide the sensitivities of  $E$  to precipitation deficits and land cover change.

evaporation, vegetation evaporation, and vegetation transpiration; the latter is a process that couples with carbon uptake through photosynthesis.

[3] The influence of  $\lambda E$  on atmospheric processes [Pielke *et al.*, 1998] has been frequently recognized [Kanemasu *et al.*, 1992; Rind *et al.*, 1992] and has been estimated using land surface models (LSMs) [Sellers *et al.*, 1997]. The increase in heat wave variability in central and eastern Europe has also been attributed to changes in  $E$  [Seneviratne *et al.*, 2006]. Summer precipitation ( $P$ ) over Europe has been linked with local  $E$  [Zveryaev and Allan, 2010]. Land surface feedbacks have also been found to increase Sahel rainfall variability both on interannual and interdecadal time scales [Zeng *et al.*, 1999].

[4] Provided that the energy storage by the canopy is negligible,  $\lambda E$  can be calculated as a residual of the surface net radiation ( $R_n$ ), the sensible heat flux ( $H$ ), and ground heat flux ( $G$ ),

$$\lambda E = R_n - H - G, \quad (1)$$

where  $R_n$  is determined from the sum of incident downward and upward shortwave and longwave radiation,

$$R_n = R_s - R_{su} + R_{ld} - R_{lw}, \quad (2)$$

<sup>1</sup>State Key Laboratory of Earth Surface Processes and Resource Ecology, College of Global Change and Earth System Science, Beijing Normal University, Beijing, China.

<sup>2</sup>Department of Geological Sciences, University of Texas at Austin, Austin, Texas, USA.

Corresponding author: K. Wang, State Key Laboratory of Earth Surface Processes and Resource Ecology, College of Global Change and Earth System Science, Beijing Normal University, 19 Xinjiekouwai St., Beijing 86-100875, China. (kewang@bnu.edu.cn)

对全球陆地蒸散的基础理论、观测方法、卫星遥感方法、以及模式模拟方面的研究进展进行了全面系统的综述。

论文约有5万字，54页，引用了662条参考文献，可以从期刊网站免费下载。

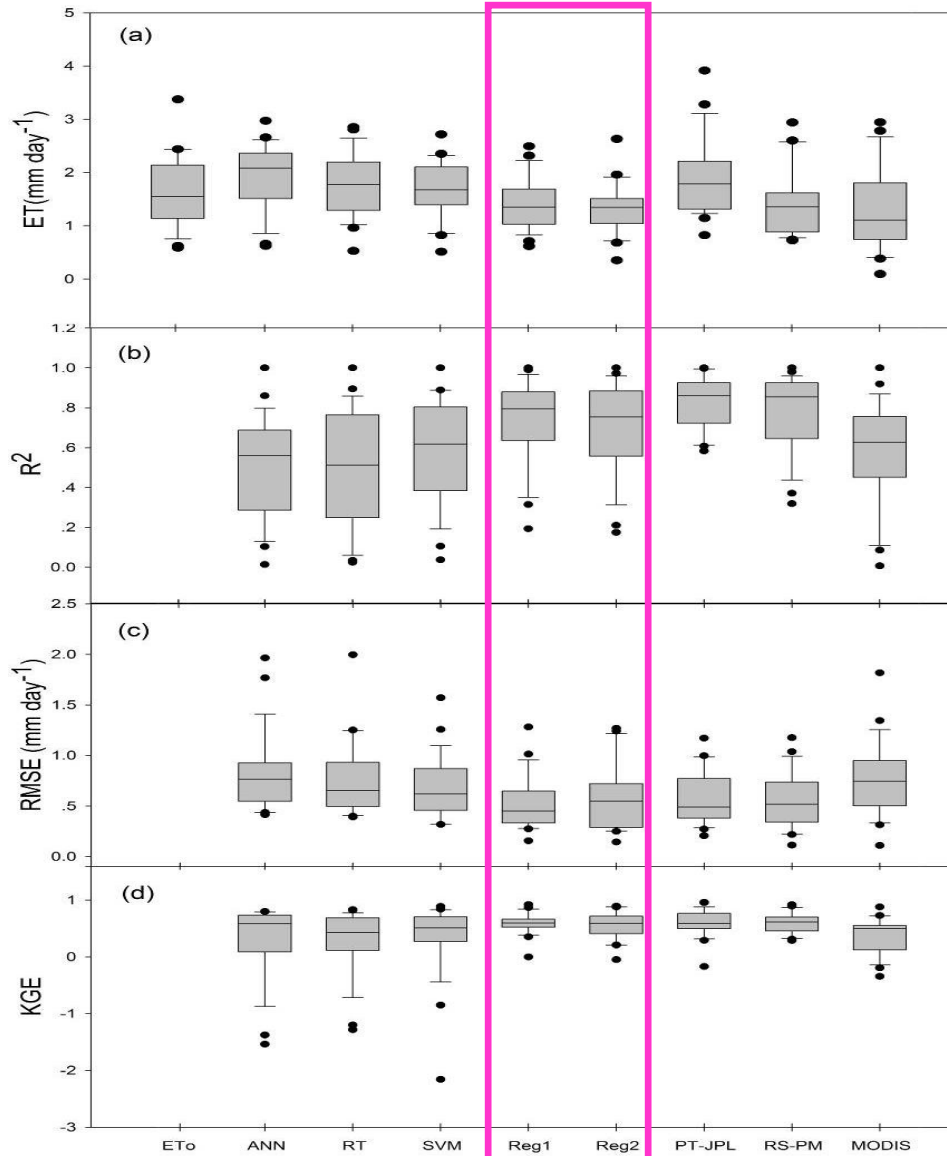
目前已经被 PNAS, Nature Geoscience, RG等著名期刊引用超过20次。



# 计算陆地蒸散的长期变化 需要联合使用气象和卫星遥感数据

- 利用全球（主要是北美）通量网的观测数据发展了一个半经验的Penman-Montieth公式来计算日平均陆地蒸散。
- 输入数据包括太阳辐射、气温、风速、相对湿度和植被指数。均为容易获取的数据，因此可以容易应用到区域或全球尺度。
- 风速对蒸散的日变化和季节变化的影响较小，但近几十年风速有明显降低，可能对蒸散的长期变化有重要影响。该模型是目前唯一显性考虑风速并能够应用到全球的陆地蒸散模型（Chen et al., 2014）。

# 在中国区域23站的独立验证



Wang et al. 开发了多个卫星遥感反演陆地蒸散的模型。

Chen等利用我国干旱和半干旱区23个站的蒸散观测，对全球现有卫星遥感蒸散模型进行了检验，Wang et al. 开发的经验模型（Reg1 和Reg2）比过程模型精度更高，且可无需局地校准，安全地应用到中国地区。

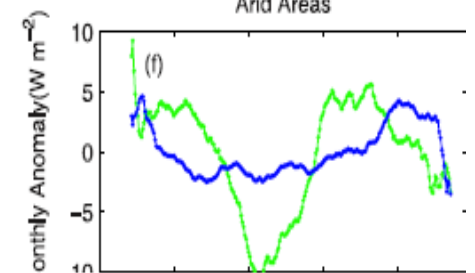
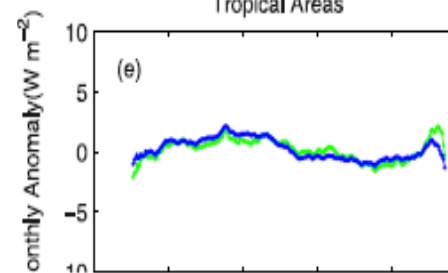
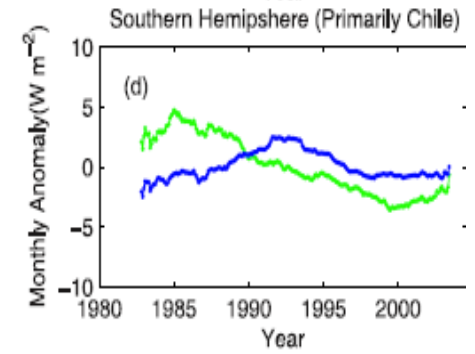
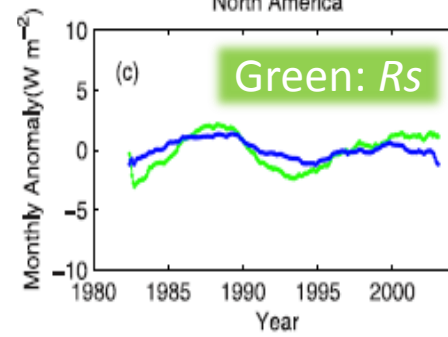
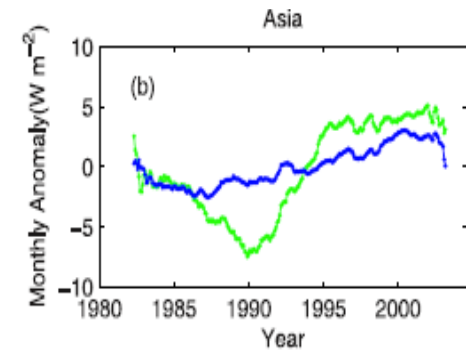
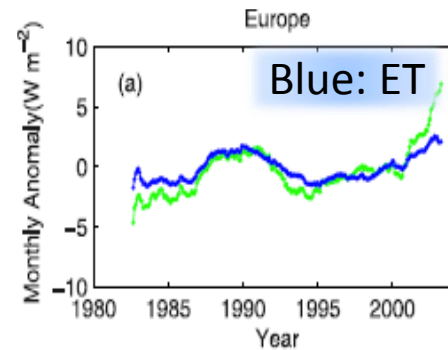
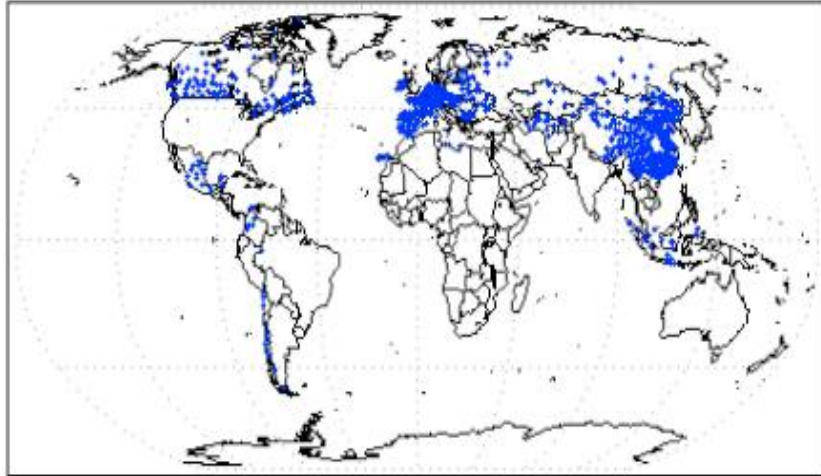
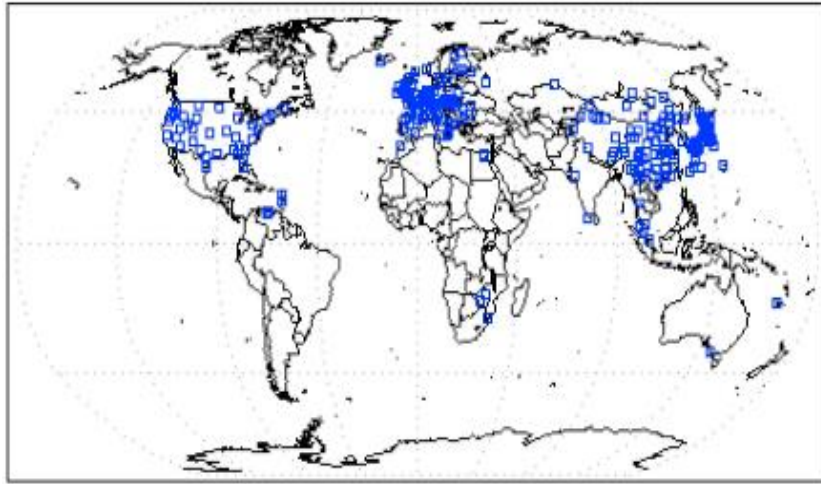
Chen et al., Remote Sens. Environ, 2014

# 在欧洲、美国、加拿大等54个站点独立验证

	Fisher	Mu	N95p	N95s	SEBS	SW	Wang	Yuan	Sun
R <sup>2</sup>	0.58	0.39	0.55	0.58	0.56	0.57	0.66	0.36	0.65
RMSE	68.5	95.3	91.5	93.1	99.8	66.6	62.9	98.1	75.4
Bias	8.9	-52.6	42.4	56.2	52.0	4.0	17.0	-54.7	3.8

以观测数据作为输入进行验证比较，Fisher和Wang的表现比较均衡，在各地都有相对较高的精度，没有明显偏差；在应用PT模型时，对PT系数做较好的限定，能取得不错的计算结果。SUN和SW模型引入了土壤湿度，从各类统计变量来看，具有较高精度，但散点图看高值偏低，低值偏高。

# 1982-2002年间陆地蒸散增加 $1.2 \text{ W m}^{-2}$ 或 $15 \text{ mm yr}^{-1}$ ( $\sim 2.2\%$ ) (Wang et al., JGR, 2010b)



# IPCC 第五次评价报告的引用和评价

Final Draft (7 June 2013)

Chapter 2

IPCC WGI Fifth Assessment Report

Since AR4 gridded datasets have been developed that estimate actual evapotranspiration from either atmospheric forcing and thermal remote sensing, sometimes in combination with direct measurements (e.g., from FLUXNET, a global network of flux towers), or interpolation of FLUXNET data using regression techniques, providing an unprecedented look at global evapotranspiration (Mueller et al., 2011). On a global scale, evapotranspiration over land increased from the early 1980s up to the late 1990s (Wild et al., 2008; Jung et al., 2010; Wang et al., 2010) and Wang et al. (2010) found that global evapotranspiration increased at a rate of  $0.6 \text{ W m}^{-2}$  per decade for the period 1982–2002. After 1998, a lack of moisture availability in SH land areas, particularly decreasing soil moisture, has acted as a constraint to further increase of global evapotranspiration (Jung et al., 2010).

**全球范围内，从20世纪80年代初至20世纪90年代后期陆地蒸散增加(Wild et al., 2008; Jung et al., 2010; Wang et al., 2010)。**

**Wang et al. (2010)发现1982-2002年间全球陆地蒸散以 $0.6 \text{ W m}^{-2}$  per decade的速度增加。1998年以后，南半球水量的缺乏，特别是土壤水分的减少，限制了全球陆地蒸散的进一步增加。**

# 小结

- 能量收支是决定气候变化的重要因子。目前，我们对大气顶的能量平衡有较好的估计。但是地表温度变化在很大程度上取决于各种气候反馈。
- 这些反馈效应具有不同的时间尺度，使得地表能量平衡更为复杂。因为缺乏有效的观测，目前我们对地表能量平衡的估计具有很大的不确定性。
- 太阳辐射的亮化和暗化受观测仪器与观测方式的影响，并且具有明显的城市偏差。
- 地表太阳辐射的变化对过去百年有较小的降温作用。
- 大气长波辐射、陆地蒸散在过去20-30年可能增加，但对具体增加幅度的估计有较大不确定性。



# 谢谢大家

Email: [kcwang@bnu.edu.cn](mailto:kcwang@bnu.edu.cn)

电话: 010-58803143

论文下载: [https://www.researchgate.net/profile/Kaicun\\_Wang/](https://www.researchgate.net/profile/Kaicun_Wang/)